# Development and testing of the HYPE (Hydrological Predictions for the Environment) water quality model for different spatial scales

Göran Lindström, Charlotta Pers, Jörgen Rosberg, Johan Strömqvist and Berit Arheimer

## ABSTRACT

The HYPE model is a hydrological model for small-scale and large-scale assessments of water resources and water quality, developed at the Swedish Meteorological and Hydrological Institute during 2005–2007. In the model, the landscape is divided into classes according to soil type, land use and altitude. In agricultural lands the soil is divided into three layers, each with individual computations of soil wetness and nutrient processes. The model simulates water flow and transport and turnover of nitrogen and phosphorus. Nutrients follow the same pathways as water in the model: surface runoff, macropore flow, tile drainage and outflow from individual soil layers. Rivers and lakes are described separately with routines for turnover of nutrients in each environment. Model parameters are global, or coupled to soil type or land use. The model was evaluated both by local calibrations to internal variables from different test basins and to data on discharge and nutrients from a large number of small basins. In addition, the estimated parameters were transferred to two larger basins in southern Sweden: River Rönneå and River Vindån. The resulting simulations were generally in good agreement with observations.

**Key words** | high resolution, hydrological model, modelling system, nutrients, scenarios, spatially distributed

**Göran Lindström** (corresponding author)
**Charlotta Pers**
**Jörgen Rosberg**
**Johan Strömqvist**
**Berit Arheimer**
SMHI,
SE-601 76, Norrköping,
Sweden
E-mail: *goran.lindstrom@smhi.se*

## INTRODUCTION

Several integrated models describing fluxes of nutrients in catchments have been developed during the last decades, e.g. HBV-N (Hydrologiska Byråns Vattenbalansavdelning, Arheimer & Brandt 1998), MONERIS (MOdelling Nutrient Emissions in RIver Systems, Behrendt *et al.* 2002), INCA-N/P (Integrated Nitrogen in Catchments, Wade *et al.* 2002*a*; Dean *et al.* 2009), SWAT (Soil and Water Assessment Tool, Arnold & Fohrer 2005) and SWIM (Soil and Water Integrated Model, Krysanova *et al.* 2005). In environmental surveys it is important to separate the contributions from various sources and to distinguish between natural variability and anthropogenic impact to enable cost-effective management practices in river basins. In general, a significant part of riverine nutrients originates from non-point sources. It would be difficult to assess the soil leaching and transport of nutrients in catchments based only on spatially scarce measurements; consequently, some kind of model must be applied. Dynamic transport models are often based on a hydrological model, as nutrient release processes are closely linked to hydrology and most of the load variability is an effect of hydrological variability. As a consequence, many of the frequently used hydrological models also have a nutrient routine linked to them (e.g. Singh 1995).

Many hydrological models were developed during the 1970s for discharge forecasts at specific sites. The HBV model (Bergström 1976) and the NAM model

doi: 10.2166/nh.2010.007

(Nielsen & Hansen 1973) are two such examples, developed for Scandinavian conditions. These water balance models were originally lumped in space, but divided into hydrological compartments. They were easy to apply, robust and transparent. However, they lacked explicit descriptions of water flow paths in the soil and water mixing in rivers and lakes. They described the energy pulse of water through catchments, but not the transport of water molecules. The shortcomings of using such models for nutrient transport became obvious in the recent development of the HBV-P model (Andersson *et al.* 2005) in which the hydrological model output was assigned to different flow paths, recalculated and linked to field-scale models. This resulted in a complicated nested modelling system that was difficult to handle, understand and calibrate.

Another difficulty when using traditional conceptual rainfall-runoff models for water quality assessments is the lack of spatial distribution. Spatial heterogeneity is essential for the water quality signal, as concentrations may vary considerably both horizontally in the landscape and vertically in the soil profile. The part of a catchment that contributes at a specific moment may strongly influence the concentration at the outlet. In addition, the mosaic itself will influence the outlet load as the mixture of sources and sinks along the water flow path will give the final integrated outcome. Water quality models have been shown to be useful tools for finding hotspots of nutrient leaching, and to identify cost-effective measures and their allocation (e.g. Arheimer *et al.* 2005). However, for such assessments the models must be spatially distributed so that they describe differences between different parts of a catchment.

The hydrological models developed during the 1970s were designed and programmed according to the input data that was available at that time. The models have not been able to fully benefit from the new spatial databases and methods that have been developed since then. Moreover, the modelling technique generally included much manual work when large-scale high-resolution applications were made. One example of such an application is the Swedish national modelling of nutrient transport, retention and source apportionment (TRK system) for reporting to the HELCOM pollution load compilations (e.g. Brandt & Ejhed 2002; Brandt *et al.* 2008).

When the EU Water Framework Directive (WFD) was about to be implemented in Sweden, it became obvious that water authorities would need detailed hydrological and hydrochemical information. The application of the WFD criteria in Sweden will probably lead to the identification of about 40,000 water bodies, with an average discharge area of the order 10 $km^2$. Scenario tools for more efficient nutrient control have been requested, since eutrophication was recognized as the most severe problem of inland and coastal waters. Some specific requirements of a model for the intended applications are realistic descriptions of flow paths and turn-over of water and nutrients. It should be able to use geographical information on e.g. soil type, land use and topography to improve the extrapolation to un-gauged basins.

Evaluations of already existing models showed that they did not fulfil all requirements, or did not have an optimal design for Swedish environmental conditions or questions asked by Swedish stakeholders. For instance, a large part of the bedrock is covered by rather thin till soils, and the number of lakes and mires is high. In addition, for a national institute such as the Swedish Meteorological and Hydrological Institute (SMHI) with the responsibility of hydrological modelling, it is important to have a flexible system, good documentation and good knowledge of the model and its behaviour.

It was therefore decided to develop a new hydrological modelling tool at the SMHI with special focus on: (1) high spatial resolution; (2) nutrient processes; (3) predictions in un-gauged basins (since monitoring would obviously not be performed everywhere); (4) a comprehensive, time effective, high computational system that fits into the operational SMHI infrastructure. The hypothesis was that this was feasible using existing knowledge and available databases. This paper describes the development and structure of the model and gives examples of applications. The new model was finally called HYPE, a model for HYdrological Predictions for the Environment.

## METHODS AND MATERIAL

### Model development

The development of the new model was carried out during the period 2005–2007. The starting point was experience of

HBV applications (e.g. Bergström 1976; Lindström *et al.* 1997); HBV-NP models (e.g. Andersson *et al.* 2005; Arheimer *et al.* 2005; Lindström *et al.* 2005) and parts of the HYPE model are based on these models. The philosophy in the model development was to start with simple process descriptions and, as far as possible, maintain a similar level of detail and complexity throughout the model. Further model refinement and increased complexity should only be introduced when necessary (e.g. Bergström 1991; Beven 2001).

The model development plan was presented by Pers *et al.* (2006). The focus during the first year was to build a flexible modelling system, in which different hydrological models could be formulated and tested, and to develop and apply a water balance model for all of Sweden within this system. The modelling system, written in FORTRAN95, was referred to as HYSS (HYdrological Simulation System). A number of different routines for optimization and sensitivity analyses, e.g. Monte Carlo simulations, were included in the system. A water quality framework was added during the second year of the project, together with simple routing through rivers and lakes. Nutrient turn-over processes and a regional groundwater flow component were added during the last year. The locations of the test basins for which results are included in this paper are shown in Figure 1. The Vindån basin (Figure 1) had been chosen for the final high-resolution application of the water quality model. Campaign measurements of discharge, water stage and nutrients were carried out during the project in Vindån to obtain data for a small-scale spatial evaluation.

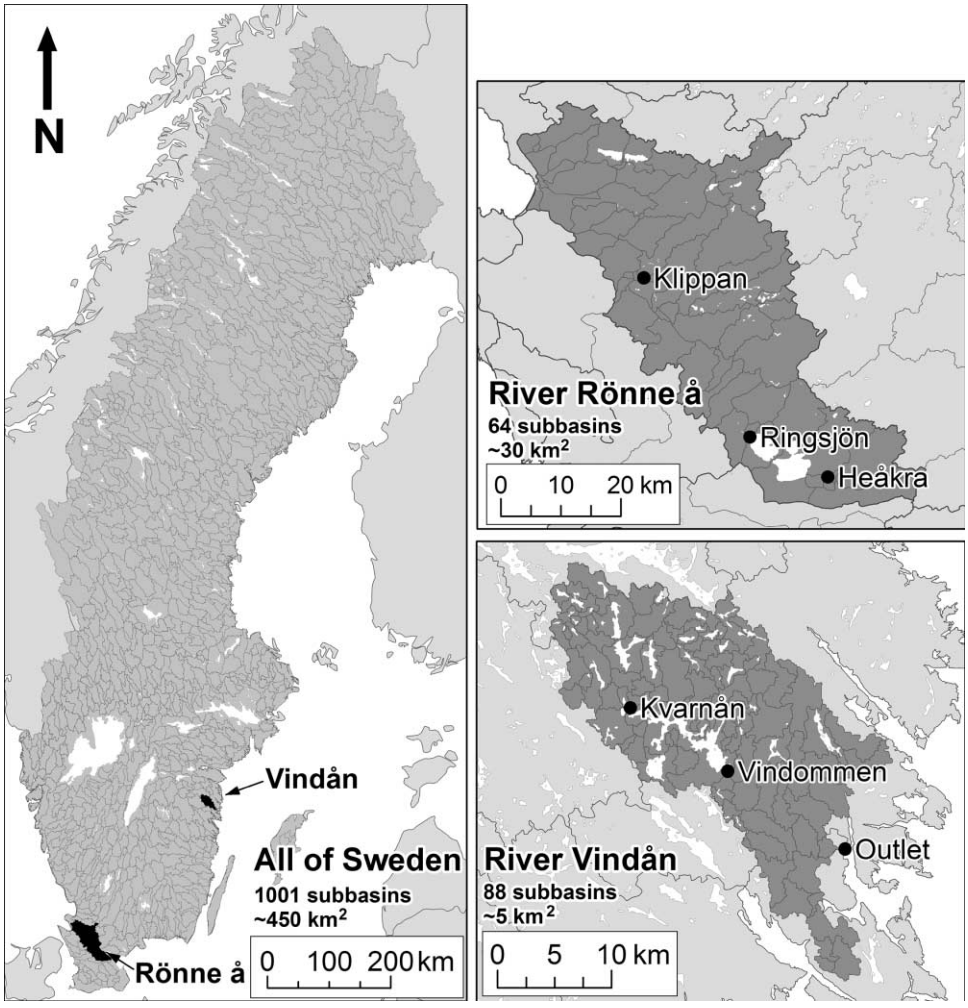


**Figure 1** | Main test basins and sampling points for which results are shown and the spatial resolution in the applications.

## Model structure

### General characteristics

In a HYPE model application, the model domain may be divided into sub-basins (Figure 2, left). Sub-basins can either be independent or connected by rivers and a regional groundwater flow. Each sub-basin can in turn be divided into classes (examples in Figure 2), which are the smallest computational spatial unit. The classes are not coupled to geographic locations, but defined as a fraction of a sub-basin area. They correspond to the hydrological response units by Flügel (1995), but also to the zones for vegetation and elevation that have always been used in the HBV model (Bergström 1976).

Land and lake classes are treated differently. Land classes are different combinations of soil type and land use. Classes may also be used as elevation zones to account for different temperature and snow conditions within a sub-basin (e.g. sub-basin S1 in Figure 2). Different vegetation types, e.g. forests and crops, are simulated as separate land uses. The area of a crop is constant during the simulation period, which means that crop rotation cannot be simulated. In a typical application a division into three soil types (e.g. clayey soils, coarse soils and till soils) and ten land uses might be used. The soil in each land class is divided vertically into one or several (maximum three) layers, which may be given different thicknesses. Such a division is for instance used in agricultural areas where a vertical resolution of processes is needed. Sub-basin S2 in Figure 2 has three classes with different soil depth, while sub-basin S3 has layered soil for different soil types and land uses. Many of the parameters in the model are coupled to soil type or land use, while others are assumed to be general to a larger region. Simulations are made with a daily time step, and the equations in the model are solved explicitly with the same time step. Simulations start from a standard initial state, and a warm-up period of typically one year is omitted from evaluations.

The model simulates concentrations in water of inorganic (IN) and organic (ON) nitrogen and dissolved (SP) and particulate (PP) phosphorus. In addition, it computes total nitrogen (TN) and phosphorus (TP) as the sum of the fractions. Other nitrogen and phosphorus fractions are also simulated within the soil, but the runoff

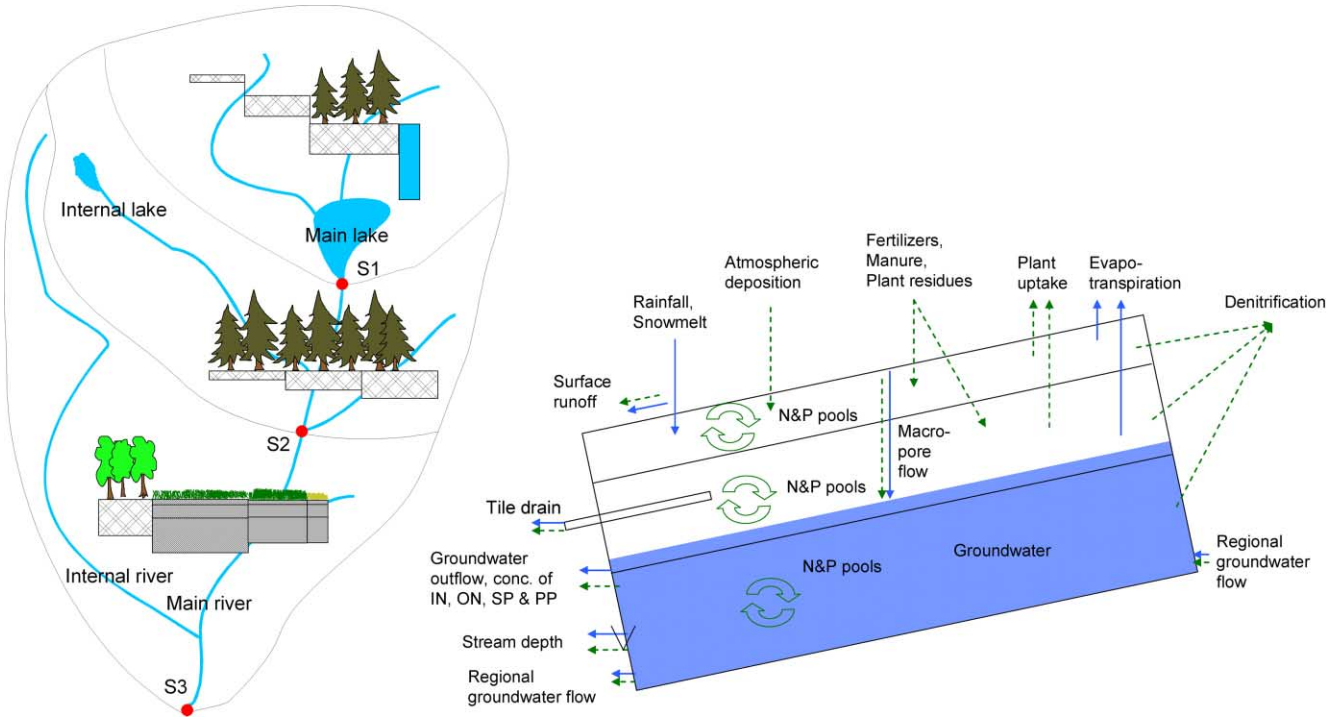


**Figure 2** | Left: schematic division into sub-basins and land classes according to elevation, soil type, vegetation and lake classes. Right: schematic model structure within a land class (i.e. a combination of a soil type and a crop), simulated using three soil layers. Solid and dashed arrows show fluxes of water and elements, respectively.

leaving the soil only contains the nutrient fractions mentioned above. Initial values of the soil nutrient pools are land-use dependent and have to be supplied by the user. The initial values for the relatively small fast turnover pools are homogenous with depth while the slow turnover pools decrease exponentially with depth. Conservative tracers can also be modelled. A more detailed description of the processes in the model is given below. All equations are found in the Appendix.

The computer code is structured to gather the hydrological processes in a section that can easily be exchanged. The model only uses a maximum of ten input data files, independent of size and resolution of domain. These input data files can easily be constructed by common software, which are also used for visualization of output data. This means that the model can be used without a user interface. The computation time depends on the complexity of the application, but the simulations presented in this paper were all carried out on a normal PC with run times of less than ten minutes.

## Snow accumulation and melt

Sub-basin mean values of daily temperature and precipitation are required as input to the model. The routine for snow accumulation and snow melt is a simplification of the HBV routine. For land classes precipitation is assumed to fall as snow below an air temperature threshold. The air temperature depends on the elevation of the class. For temperatures within an interval around the threshold, a mixture of rain and snowfall is assumed (Equation (1), Appendix). Snow is accumulated for each land class until melting. Snow melt is calculated with a degree-day method, and uses the same threshold temperature as snowfall (Equation (2), Appendix). The degree-day parameter depends on land use. Storage and refreezing of meltwater and rainfall in the snow pack is disregarded.

## Water flow in the soil

A fraction of the rainfall and snowmelt infiltrates into the topsoil (Equation (3), Appendix), and the remainder is diverted to surface flow and flow through macropores. Flows are diverted only if the incoming water and the soil moisture in the uppermost soil layer exceed threshold values (Equations (4) and (5), Appendix). Both diverted flows depend on soil type and are calculated as fractions of the incoming water above the threshold. Macropore flow primarily enters the soil layer in which the groundwater table is located. If the maximum water content of this layer is exceeded, the remaining water is stored in the layer(s) above. If the soil moisture in the uppermost soil layer exceeds the maximum water content, saturated overland flow occurs. It is calculated as a part of the excess water and is dependent on land use (Equation (6), Appendix).

The maximum water content of a soil layer is determined by three model parameters coupled to soil type and soil layer: the fraction not available for evapotranspiration, the fraction available for evapotranspiration but not for runoff and the fraction available for runoff (Figure 3). The sum of the three parameters comprises the maximum water content of the soil (i.e. the total porosity of the soil). The first two fractions roughly correspond to the concepts of wilting point and field capacity, which in principle could be measured. These terms have been avoided here, however, since there is no guarantee that measured values can be applied directly in the model. Soil moisture above the threshold determined by the fraction of water available for runoff may percolate down to the next layer. The percolation is limited by a soil type dependent on maximum percolation capacity and by the available space in the soil layers below (Equation (7), Appendix). If the maximum water content of a soil layer is reached, that soil layer is considered saturated.

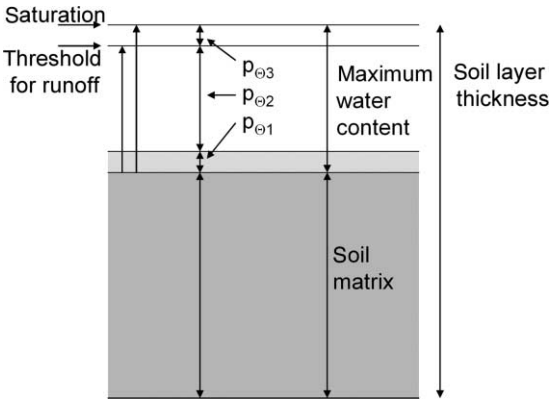


**Figure 3** | Definitions of water-holding parameters for a soil layer.

Evapotranspiration may occur from the two top soil layers; the depth of the second soil layer can therefore be considered as the plant rooting depth. Evapotranspiration is assumed potential if the soil moisture is above a certain threshold, and decreases linearly from that threshold to the threshold for evapotranspiration where it is zero. Potential evapotranspiration depends on temperature and a seasonal adjustment factor. The seasonal adjustment factor increases the evapotranspiration in spring and decreases it during autumn. It is zero for temperatures below a threshold value (as for snow fall and snow melt). Evapotranspiration is assumed to decrease with depth. It is divided between the two layers based on evaluations of a decreasing exponential function at the midpoint of each layer (Equation (8), Appendix).

The depth to the groundwater table is quite small in most Swedish soils (typically in the order some metres). There is therefore no separate compartment for groundwater in the model. Instead, the soil water content in the individual soil layers determines the existence of a groundwater level. The groundwater table is located in the uppermost layer with excess water. This excess water also defines the groundwater level within a soil layer. It is therefore, in principle, possible to have a perched groundwater table. Excess soil water can drain from any soil layer located fully or partly above the stream depth, if the soil moisture in that layer exceeds the threshold for runoff. This runoff is a fraction of the excess water determined by runoff coefficients (Equation (9), Appendix). In the soil layer where the stream depth is located, only the part of the excess soil moisture above the stream depth is included in the calculation. The runoff coefficients are coupled to the type, depth and slope of the soil. Tile drains are optional in the model and the presence and depths of these are determined by the user for each land class. The runoff from tile drains is determined by the groundwater level above the tile depth and a soil type dependent recession coefficient (Equation (10), Appendix). The runoff is abstracted from the soil moisture in the layer in which the tile is located, and is limited to the soil moisture above the threshold for runoff in that layer. The discharge from the soil, tile drains and surface runoff are directed to the stream. Flow is disregarded in the unsaturated part of the soil layers.

Regional groundwater flow can be simulated, and is determined by a recession coefficient (Equation (11), Appendix). This flow is taken from the bottom soil layer of each land class (if the soil moisture in that layer exceeds the threshold for runoff). The water may be transported to a lake at the sub-basin outlet and/or to the soil of the next sub-basin. The regional groundwater flow is added to the bottom soil layer of each land class of the receiving sub-basin. If these layers become saturated, however, the excess water is added to the layers above.

### Rivers and lakes

There are two types of rivers and lakes in the model (Figure 2), referred to as internal and main rivers and lakes. The internal rivers and lakes only receive local runoff from the sub-basin. They are lumped together into one river and one lake, which are connected in series. The lake can be bypassed by a fraction of the local runoff. The second type, main rivers and lakes, constitutes the coupling between sub-basins. These rivers and lakes receive the local runoff (after it has passed internal rivers and lakes) and the river flow from upstream sub-basins. Bifurcations can be treated by dividing the outflow from a sub-basin into two receiving sub-basins.

Lakes are defined as classes with specified areas, whereas the area of rivers is disregarded in relation to precipitation and evaporation. Precipitation falls directly on lake surfaces, i.e. ice and snow on lakes are not simulated, and lake water evaporates at the potential rate until the lake is dry. Each lake has a defined depth below an outflow threshold. Internal lakes are given a regional value of the depth, whereas the depth can be set individually for main lakes. The potential evaporation is calculated in the same way as for land surfaces.

The river flow is delayed in time, according to the river length and a flood wave velocity. The river lengths are approximated as the square root of the sub-basin area, if not given as input. In addition to the delay, the flow can also be attenuated. The attenuation part of the delay is realized through damping in a linear reservoir with a recession coefficient which approximately gives the required delay (Equation (12), Appendix).

The outflow from internal lakes is determined by a rating curve, which is the same for all internal lakes in the

model application. The outflow from main lakes is also determined by this general rating curve unless a specific one is given or if the lake is regulated. Lakes and man-made reservoirs are not separated in the simulation. A simple regulation rule can be used, in which the outflow is constant or follows a seasonal function for water levels above the threshold. A rating curve for the spillways can be used when the reservoir is full (Equation (13), Appendix).

### Additional hydrological variables

Snow depth is estimated from the water content of snow and a snow density factor which increases with the average age of the snow pack (Equation (14), Appendix). The soil temperature is a weighted sum of the air temperature, the soil temperature previous day and a constant deep soil temperature. The influence of air temperature decreases with increasing snow depth. The soil frost depth is finally a function of soil moisture and the soil temperature. The calculations of soil temperature, soil frost and snow depth are taken from Lindström *et al.* (2002).

### Nutrients in the soil

Within the soil, nitrogen and phosphorus are divided into mobile and immobile nutrient pools (Figure 4). The different pools and the processes affecting nutrients in the HYPE model are similar to those of other nutrient models, e.g. SOIL-N (Johnsson *et al.* 1987), ANIMO (Groenendijk & Kroes 1999) and ICECREAM (Tattari *et al.* 2001). Some alterations, often simplifications, have however been made to fit the general complexity level and the scope of the HYPE model.

For nitrogen, the simulated pools (Figure 4) consist of a slowN pool, a fastN pool and an inorganic N pool (IN pool). The slowN pool represents the organic nitrogen in the soil with a long turnover time. From the slowN pool, nitrogen is released to the fastN pool through degradation processes. The fastN pool represents the organic nitrogen in the soil with a short turnover time. Nitrogen in this pool is available for mineralization in which it is transferred into the inorganic N pool. These two processes are determined by the available amount of substrate, the soil temperature

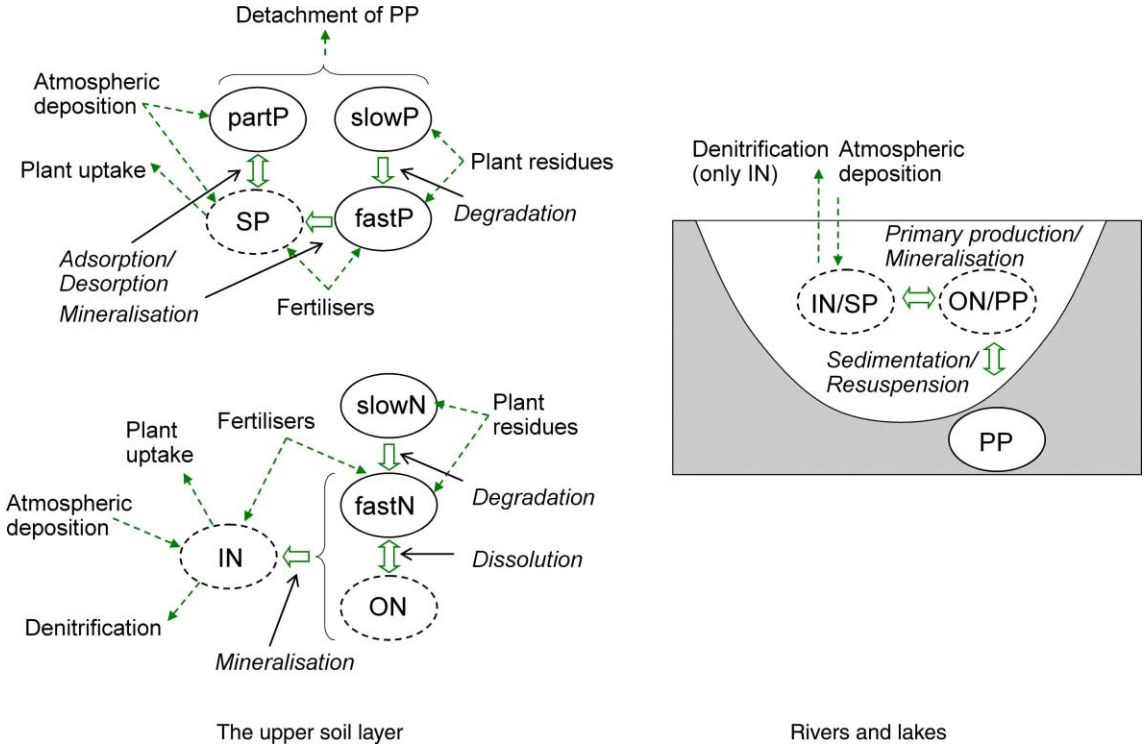


**Figure 4** | Nitrogen and phosphorus processes in the upper soil layer, rivers and lakes, and the nutrient fractions simulated (IN-inorganic nitrogen, ON-organic nitrogen, SP-dissolved phosphorus, PP-particulate phosphorus). Mobile pools are in broken lines; immobile pools in solid lines.

and soil moisture. Denitrification is a sink of inorganic nitrogen in all soil layers, increasing with increasing soil temperature, soil moisture and IN content of the soil. Details of soil pool transformation processes are found in Equation (14) of the Appendix. All nitrogen in the IN pool is considered to be mobile and can hence be transported between soil layers or out of the profile with horizontal and lateral soil water flow. The concentration of organic nitrogen in soil water is determined by the fastN pool. The mass transfer of nitrogen between the fastN pool and ON in solution is driven by the difference between the ON concentration in the soil solute and a steady-state equilibrium concentration calculated from the total nitrogen content of dissolved organic nitrogen and the fastN pool (Equation (15), Appendix).

As for nitrogen, phosphorus in the soil (Figure 4) is divided between a slow turnover organic P pool (slowP), a fast turnover organic P pool (fastP) and a soluble inorganic pool (SP pool). However, for phosphorus a fourth pool (partP pool) is also simulated which represents P adsorbed to mineral particles. Whereas the transfers of phosphorus between the slowP and fastP pools and the fastP and SP pools are similar to the nitrogen transformations, transfer of phosphorus between the SP and partP pools is governed by adsorption and desorption processes (Equation (16), Appendix). An equilibrium sorption concentration of P in the soil solute is iteratively calculated from the total phosphorus in the two pools using the Freundlich sorption isotherm. The transfer between the pools is then driven by the difference between the SP concentration in the soil solution and the equilibrium concentration.

Vegetation extracts inorganic nitrogen and soluble phosphorus (Figure 4) in the top two soil layers (Figure 2), similar to evapotranspiration. Potential plant uptake of nutrients in the HYPE model follows logistic uptake functions with the uptake of phosphorus being proportional to the uptake of nitrogen. Actual uptake only occurs between the sowing date or the start of the growing season and the harvest date or the end of the growing season. Uptake during the main growing season is limited only by the availability of nutrients. Autumn-sown crops are limited by a temperature function during autumn to account for poorer growing conditions during this part of the year. Secondary crops such as catch crops may also be modelled. These crops have individual uptake functions and compete for nutrients with the main crop. The plant uptake functions are described in Equation (17) of the Appendix. Nutrient uptake by plants on land uses other than agricultural, for example woodland, is modelled in the same way but using other parameter sets.

### Atmospheric and land-use based nutrient sources

Sources of nitrogen and phosphorus to the soil include applied organic and inorganic fertilizers, plant residues and atmospheric deposition (Figures 2 and 4). Inorganic fertilizers and the inorganic part of manure are added to the IN and SP pools at specified fertilizer dates. The organic N and P fractions of manure are added to the fastN and fastP pools. The fertilizer and manure may be spread in equal amounts over several days to account for uncertainties and spatial variation in application dates. The fertilizers and manure are divided and added to the top two soil layers in proportions set by the user allowing for simulation of different tillage practices. Plant residues are returned to the soil on specified days in which the nutrient contents of the residues are added to the fast pools and the slow pools. As for fertilizers and manure, plant residues can be added to the top two soil layers.

Atmospheric deposition is a source of nitrogen and phosphorus to land and lake classes. Wet deposition is added as a concentration of IN and SP in precipitation. Dry deposition is land-use dependent and the nitrogen and phosphorus is added to the IN pool and PartP pools in the top soil layer for land classes and to the lake IN and PP for lake classes.

### Erosion

Particulate P losses from land to watercourses are assumed, in the model, to occur solely due to erosion of soil particles containing phosphorus. The model representation of erosion can be split into detachment and transport processes. Detachment is simulated using elements of the revised Morgan–Morgan–Finney model (Morgan 2001) where some parts are reformulated to fit the time step of the HYPE model. Sediment on the soil surface is detached by either of two mechanisms: rain splash detachment and detachment

due to the abrasive power of surface runoff. The effect of detachment due to leaf drip has been ignored in this model. Detachment of particulate P is calculated from the detached sediment and the total P content of the slowP and partP pools.

The kinetic energy of rainfall reaching non-snow-covered ground is the driving force of rain splash detachment. It depends on the rainfall amount and a constant rainfall intensity. To account for protection from vegetation cover, a crop cover factor which varies over time is calculated for each land use from two vegetation parameters. Rain splash detachment is estimated from these factors and the erodibility of the soil. The detachment due to overland flow is a function of surface runoff, slope, ground cover and the cohesion of the soil. As with crop cover, a ground cover factor is determined from two parameters specific to each vegetation type. Both the erodibility and the cohesion are soil-type-dependent parameters.

Once detached, PP is transported to a landscape storage pool with overland flow and/or with flow through macropores in connection with tile drains. The amount of detached PP that is transported to the pool is determined by the transport capacity of the flow through these pathways. Attenuation factors are applied to account for the filtering effects of the soil (macropore flow) and vegetation and other flow obstacles on the soil surface (overland flow) during the transport process. An adjustment factor is also calculated to account for enrichment of phosphorus during the erosion process.

From the landscape storage pool of each class, PP is released to the internal river of the sub-basin as a function of the size of the pool and generated soil runoff in the class. The equation for this process has been tested for transport of suspended sediment on a catchment scale (Lidén 1999). All processes describing erosion and transport processes are described in detail by the Equations (18) of the Appendix.

## Nutrients in rivers and lakes

Nitrogen and phosphorus entering rivers and lakes are affected by several processes altering the quantity and speciation of the substances (Figure 4). The processes considered in this application are: sedimentation, resuspension, primary production, mineralization and denitrification. Total mixing of the water in lakes is assumed at each time step.

Organic nitrogen and particulate phosphorus is removed from the lake water volume through sedimentation (Equation (19), Appendix). The amount of PP and ON removed at each time step is affected by the concentration of the substances in the lake and the lake area. None of the settled material in lakes is later assumed to be available for resuspension. In rivers, particulate P is redistributed over time through sedimentation and resuspension processes. Depending on the river discharge, sedimentation and resuspension are accentuated during low and high flows, respectively. This process is dependent on the water depth and bottom area of the rivers, estimated from empirical expressions. The bank full flow, approximated from the second-highest simulated daily river flow during a period of one year, is also used in the calculations.

Primary production is a process which transforms IN and SP into ON and PP in water bodies (Equation (20), Appendix). The process is reversed during mineralization. The transfer between the different pools in the model is simulated as a function of water temperature, average total phosphorus concentration and the current water temperature change. When water temperature is increasing, net primary production is assumed and when water temperature is decreasing, net mineralization is assumed. The process is active in the full river volume but only down to a specified depth in lakes. Adsorption/desorption of phosphorus to particles is also assumed to be included in this transformation.

Denitrification is a significant sink for inorganic nitrogen in lakes and rivers. It is calculated as a function of water temperature, IN concentration in the water body and lake or river surface area.

## Loads from other nutrient sources

Routines for dealing with nutrient additions from industrial, urban and rural sources are included in the model. N and P load from industrial and urban point sources (sewage treatment works) are added to the main river as a volume of water and concentrations of IN, ON, SP and PP. Nitrogen and phosphorus from rural households are added partly to the internal river of the sub-basin and partly to the deepest soil layers of the land classes in the sub-basin.

### Input data

The input data and data for calibration of the model were mainly collected from national datasets. Further studies are envisioned in order to study the sensitivity to the choice of input data. An overview of input data for the HYPE model is given in Table 1.

### Local model evaluations

To test the validity of different parts of the model, comparisons were made with observations of internal variables, e.g. snow depth and groundwater depths, and outflow variables, e.g. discharge and nutrients in the outflow. Observations from different river basins were used since there was no single site from which all the variables were available. For this model evaluation, the parameters were optimized to each particular site, variable and time period.

### Estimation of regional parameters

Local calibration cannot be made for all points of interest and therefore regional parameter values have to be estimated. Whereas some of the parameters were derived from literature values or previous model applications, many needed to be calibrated. Given the relatively large amount of parameters available for calibration in the HYPE model, it was assumed that using an automatic calibration routine on the whole set of calibration parameters was not plausible. The soft data concept (Seibert & McDonell 2002) could be useful in this context, but here a step-wise calibration of different parts of the model was made. Most parameters were calibrated manually, thus incorporating hydrological experience and knowledge, i.e. using soft data. Some parameters, however, were optimized automatically against observations of corresponding processes (e.g. snow depth and evapotranspiration). Data from a large number of basins in different parts of Sweden were used. In particular, water quality parameters were calibrated using a data set from small agricultural basins, described by Kyllmar (2004).

### Parameter transferability

The validity of the regional model parameters was tested by transferring the model to two test basins: Rivers Rönneå and Vindån (Figure 1). No local calibration was made (except for the lake parameters) and the applications are therefore examples of two almost independent evaluations. The River Rönneå is located in southern Sweden. The area of the drainage basin is approximately 1,900 $km^2$,

**Table 1** | Input data for the HYPE model

| Data type | Data | Source |
|---|---|---|
| Climatological data | Precipitation, air temperature. Daily sub-basin means | Johansson (2002) |
| Geographical data | Sub-basin areas | Swedish water archive (SMHI) |
| | Soil type | Soils database (SGU) |
| | Land use | Corine land cover |
| | Elevation, slope | GSD Terrain elevation databank (Lantmäteriet, the Swedish mapping, cadastral and land registration authority) |
| Lake information | Depths, regulation rules, rating curve | Swedish water archive (SMHI) |
| Water quality | Initial nutrient pools in soil | Eriksson *et al.* (1997) |
| Agricultural practices | Manure and inorganic fertilizer application, crop husbandry. Timing and amount for fertilization, sowing and harvesting | Statistics Sweden |
| Other nutrient loads | Rural house holds, industries, waste water treatment plants, atmospheric deposition | Statistics Sweden, Swedish Environmental Research Institute, SMED consortium |

here divided into 64 sub-basins. The fraction of agricultural land is 31%. Lake Ringsjön is located in the upper part of the catchment, and is slightly regulated. The River Rönneå drains into the Skälderviken Bay on the Swedish west coast. Most of the households in the area are connected to municipal wastewater treatment plants. The catchment is well documented and has been in focus in several previous research projects on nutrient losses and model applications (e.g. Andersson *et al.* 2005; Arheimer *et al.* 2005; Lindström *et al.* 2005; Bouraoui *et al.* 2009).

The Vindån system is located on the southeast coast of Sweden, and drains into the Baltic Sea in the Kaggebofjärden bay. The size of study area is 430 $km^2$ and includes some adjacent areas to River Vindån that all discharge into the Kaggebofjärden bay. For simplicity, it is referred to as the Vindån basin here. The total area was divided into 88 sub-basins, giving an average sub-basin size of 5 $km^2$. The fraction of agricultural land in the Vindån study area is 18%. The area has been used as a pilot basin for campaign monitoring and in previous nutrient pollution studies. The most recent study resulted in a locally suggested action plan with support from local farmers and other stakeholders (Andersson *et al.* 2008).

## RESULTS AND DISCUSSION

### Local model evaluations

Examples of results for different parts of the model are shown in Figure 5 for a selection of sites. The results were obtained by local optimization of model parameters to each particular site, variable and time period using the Nash–Sutcliffe efficiency $R^2$. The state variables snowpack and lake water level are among the most accurately simulated of the shown variables, with $R^2 > 0.9$. The diagnostic variables soil frost depth and groundwater level are also well simulated. The groundwater level simulation is a good indication of the performance of the model in simulating the soil moisture state variable. It therefore provides good confidence in this internal variable.

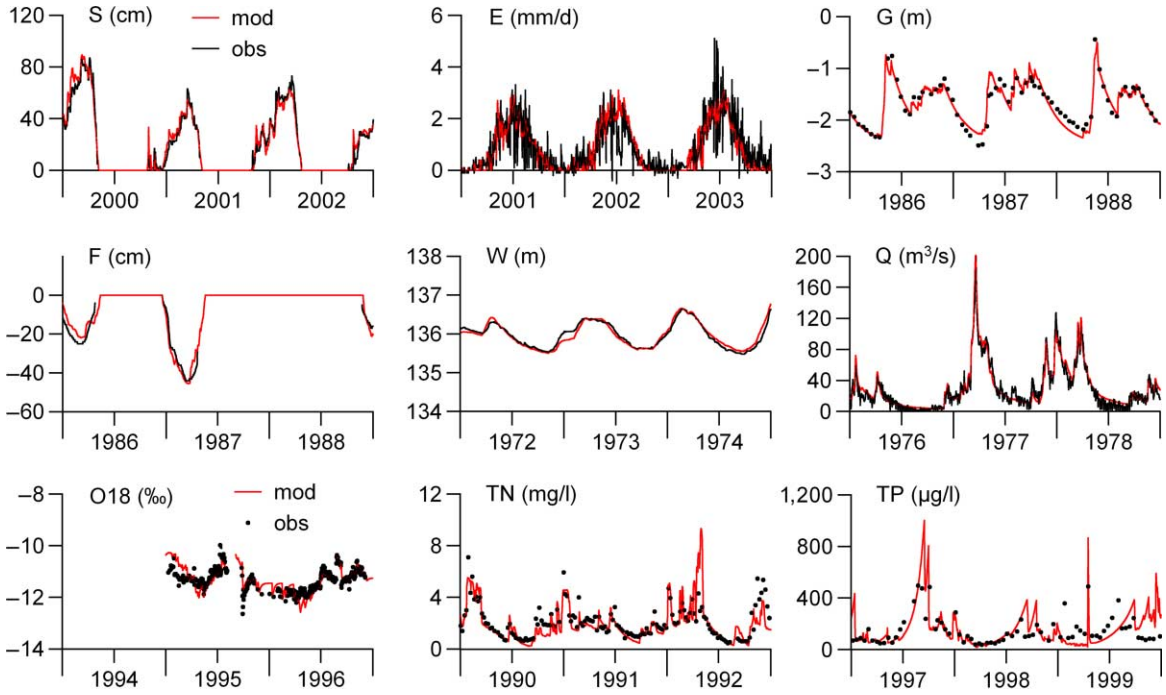


**Figure 5** | Examples of local model evaluations from different river basins in Sweden (gray: simulation and black: observations). The model was optimized to the observations in each particular diagram. S: snow depth at Ljusnedal ($R^2 = 0.92$); E: evaporation at Norunda ($R^2 = 0.59$; Grelle 2008); G: groundwater level at Svartberget ($R^2 = 0.90$); F: soil frost depth at Svartberget ($R^2 = 0.84$, Lindström *et al.* 2002); W: lake water level in Lake Möckeln ($R^2 = 0.95$); Q: discharge at Torsebro ($R^2 = 0.94$); O18: $^{18}O$ content at Stubbetorp ($R^2 = 0.54$, Andersson & Lepistö 1998); TN: total nitrogen at JRK research basin O19 ($R^2 = 0.68$) and TP: total phosphorous at JRK research basin AB5 ($R^2 = 0.41$).

The modelled evapotranspiration (Figure 5) explained slightly more than half of the variability in the measured evaporation at Norunda ($R^2 = 0.59$). The combined effect of the different parts of the model is shown by the flow and concentrations of substances. Discharge is very well captured, and the overall variation of $^{18}O$, TN and TP concentration is also simulated rather well. The simulation of groundwater levels and the conservative $^{18}O$ isotope suggest that the model describes water pathways and transit times reasonably well.

To summarize, the model could be calibrated to agree rather well with both internal variables within a basin and outflow variables. The agreement in Figure 5 is, however, probably much better than what can be expected when using regional parameter sets. The agreement in regional applications and the ability to model un-gauged basins must be studied further.

## Parameter transferability

Figure 6 shows examples of streamflow and total nitrogen from River Rönneå for three selected sites. Here the parameters obtained from the regional calibration for different sites were used. The modelled streamflow is relatively good, especially in the two small sub-basins without lakes (Heåkra and Klippan). The simulated nitrogen concentration in the agriculturally dominated Heåkra basin has a very different pattern than the Klippan sub-basin, which is mainly forested (Figure 6). During flow episodes, the groundwater level reaches the upper soil

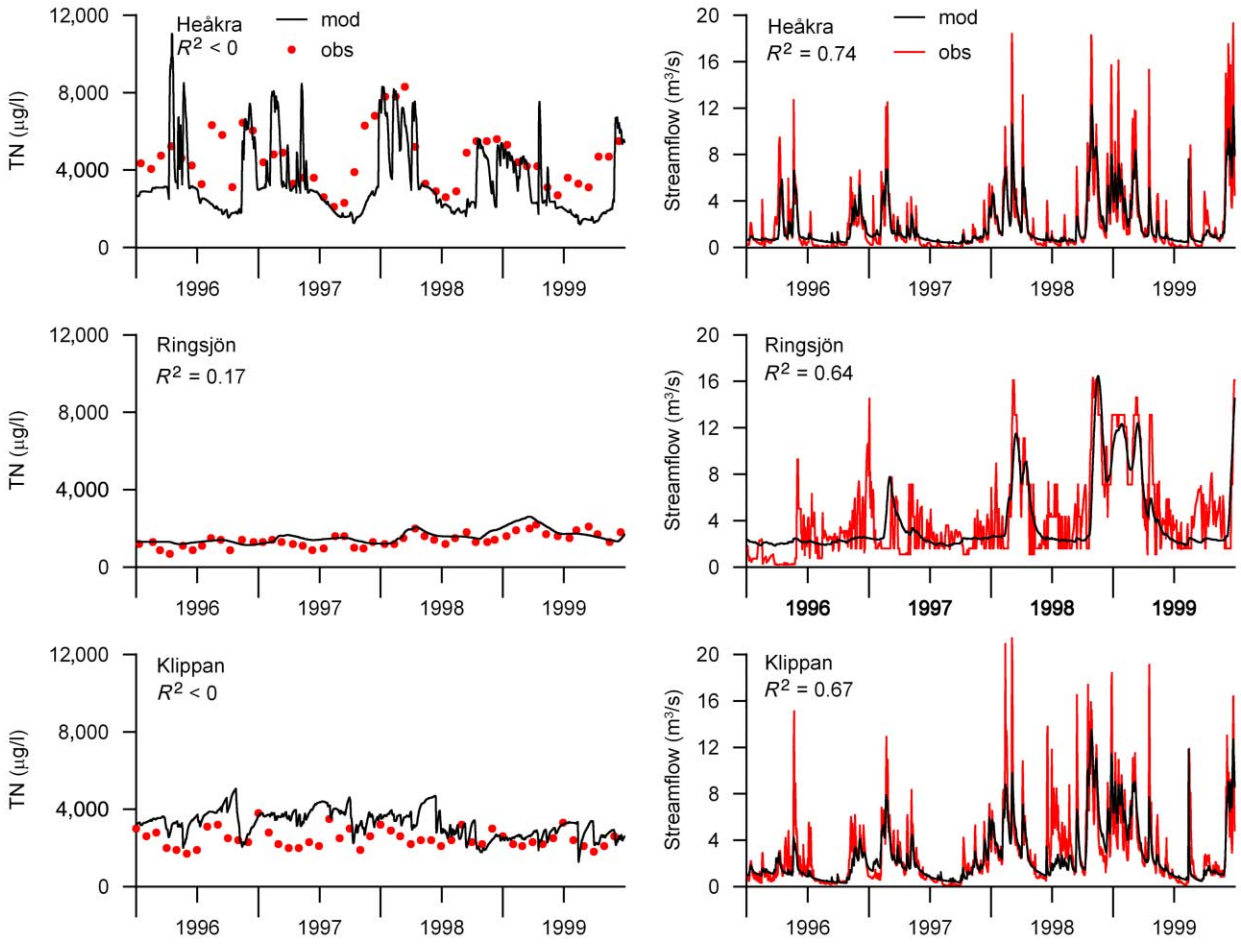


**Figure 6** | Examples of simulation results of streamflow and total nitrogen for three sites in the Rönneå River basin. Top: the mainly agricultural Heåkra; middle: the outflow from the regulated lake Ringsjön; and bottom: a mainly forested tributary at Klippan.

layers and the outflow has a high proportion of superficial water with high concentrations of nutrients. This is clearly the case in Heåkra. Forested areas, for instance Klippan, do not have this feature as only one soil layer is used there. In addition, the observed autumn increase in TN concentration in Heåkra is too late in the simulation. This could be due to groundwater level rising too late to the upper soil layer or an overestimated retention during the summer.

Figure 7 shows streamflow, water level, total nitrogen concentration and total phosphorus concentration from River Vindån, compared to some of the campaign measurements gathered in the area. The agreement is reasonable, especially considering that the model parameters were not optimized using these observations.

The outflow from lakes is smoother than river flow since the lakes dampen the flow. In both Kvarnån (which has several lakes upstream) and Lake Vindommen, the modelled discharge and water level are simulated relatively well (Figure 7). Lakes have a large impact on nutrient concentration, as can be seen in e.g. Lake Ringsjön in River Rönneå (Figure 6). The total nitrogen concentration in Lake Ringsjön is rather constant and much lower than the concentration of the inflow from the largest tributary at Heåkra, due to the retention in the lake. No calibration of the lake parameters was carried out in Vindån basin. Instead, the same lake parameter values obtained from calibration in the River Rönneå was used, with satisfactory results. This means that the HYPE model managed to simulate this basin in an un-gauged mode, and that parameters can be transferred within reasonably homogeneous regions.

The intensely monitored event in spring of 2006 at the Vindån outlet to the sea is captured well by the model. The nutrient concentration peak is caused by intense runoff from agricultural areas downstream of Lake Vindommen, while the more continuous discharge from the lake has lower nutrient levels. This feature can only be simulated by a distributed model. The HYPE model can capture the spatial resolution and its effects on nutrient dynamics in a catchment.

Figure 8 shows the spatial variation in winter (DJF) median concentrations in the Rönneå tributaries. The simulated concentration is generally better for nitrogen than for phosphorus. Total and particulate phosphorus is generally underestimated, while no clear trend is visible for soluble phosphorus. The error of simulated winter

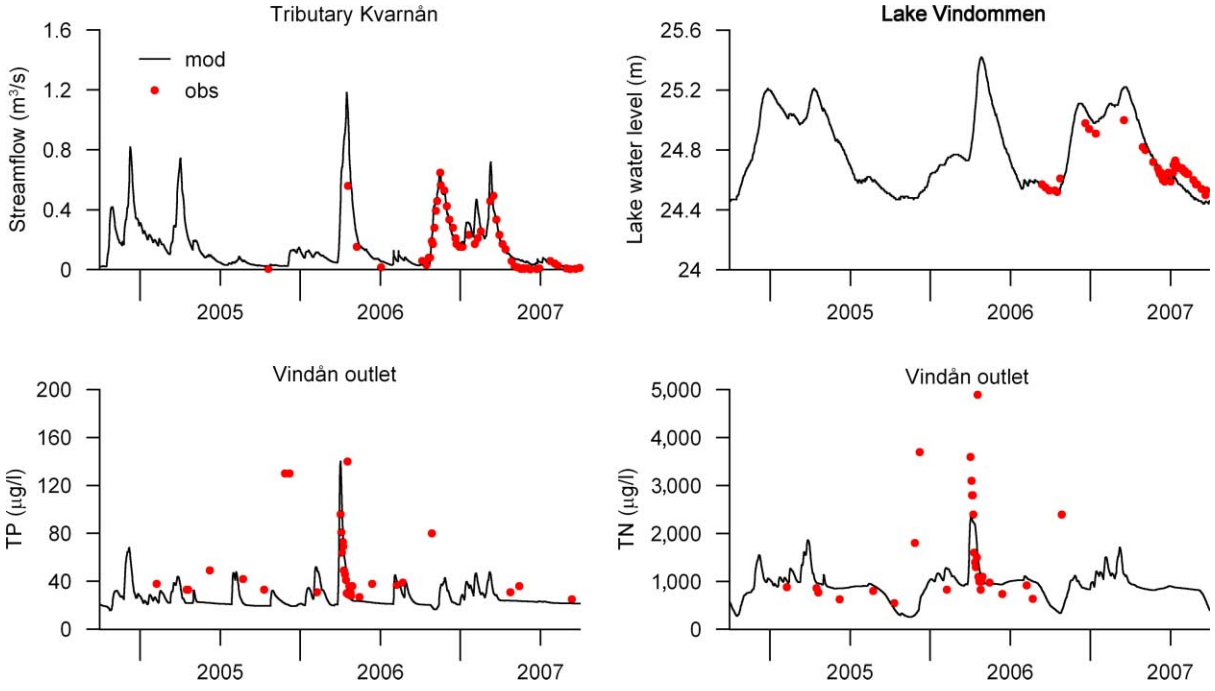


**Figure 7** | Examples of simulation results compared to campaign measurements from Vindån: streamflow in the tributary Kvarnån, water stage in Lake Vindommen, total phosphorus and total nitrogen at the outlet of Vindån into the Baltic Sea.

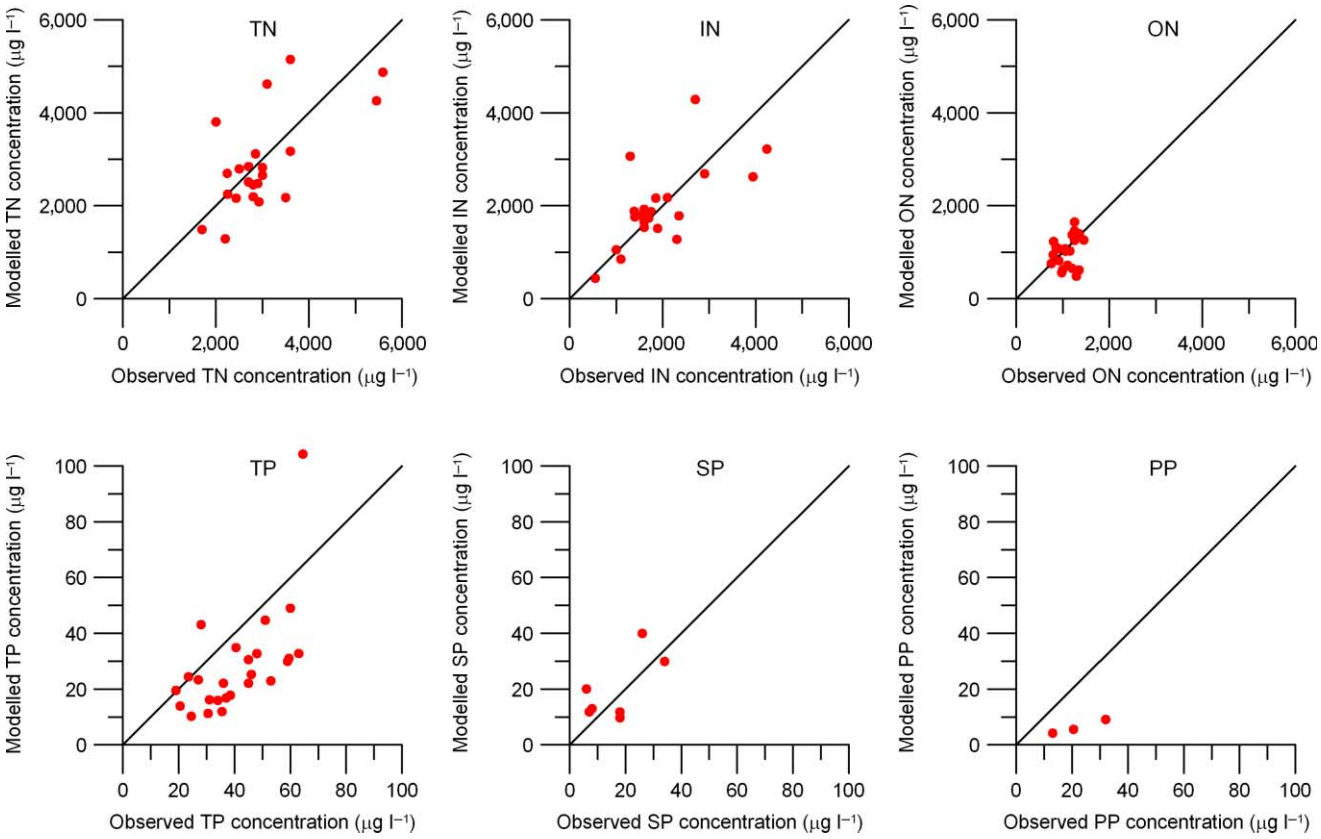


**Figure 8** | Simulated versus observed winter median concentrations of nitrogen and phosphorus in the Rönneå catchment.

concentration for specific sub-basins is quite large and there is room for further improvement in the model. The spatial variation of nutrient load in the Vindån basin is shown in Figure 9. Both nitrogen and phosphorus roughly follow the spatial distribution of agricultural land, but the spatial variability can also be attributed to differences in soil types between sub-catchments. The results show that the HYPE model managed to capture much of the spatial variation in nutrient concentrations. Average conditions can of course be mapped by much simpler means than by the use of a dynamic model, but a model can also provide information on the variation over time and prospects for predictions of the effects of different scenarios.

The fact that the model parameters are related to physiographic characteristics means that parameters are not dependent on the division into sub-basins. This improves the possibilities for transferring model parameters to un-gauged basins, and means that the model is less sensitive to the scale and resolution of the model. The intention is that the model will not need re-calibration when the horizontal resolution changes and that the model should be applicable to a wide range of scales.

## Differences between the HYPE model and similar models

Many aspects of models can be compared, such as complexity, level of process representation, data requirements, applicability, model purpose, time-consumption (i.e. cost) and performance of model results. These aspects were explored in the Euroharp project, where nine different nutrient loss models were compared and evaluated. Model comparisons were made from both a theoretical point of view (Schoumans *et al.* 2009) and of model results (e.g. Kronvang *et al.* 2009; Silgram *et al.* 2009). However, many models in Euroharp have only been used on a national or local scale or were new. The development of HYPE began with a literature review, which concluded that no available

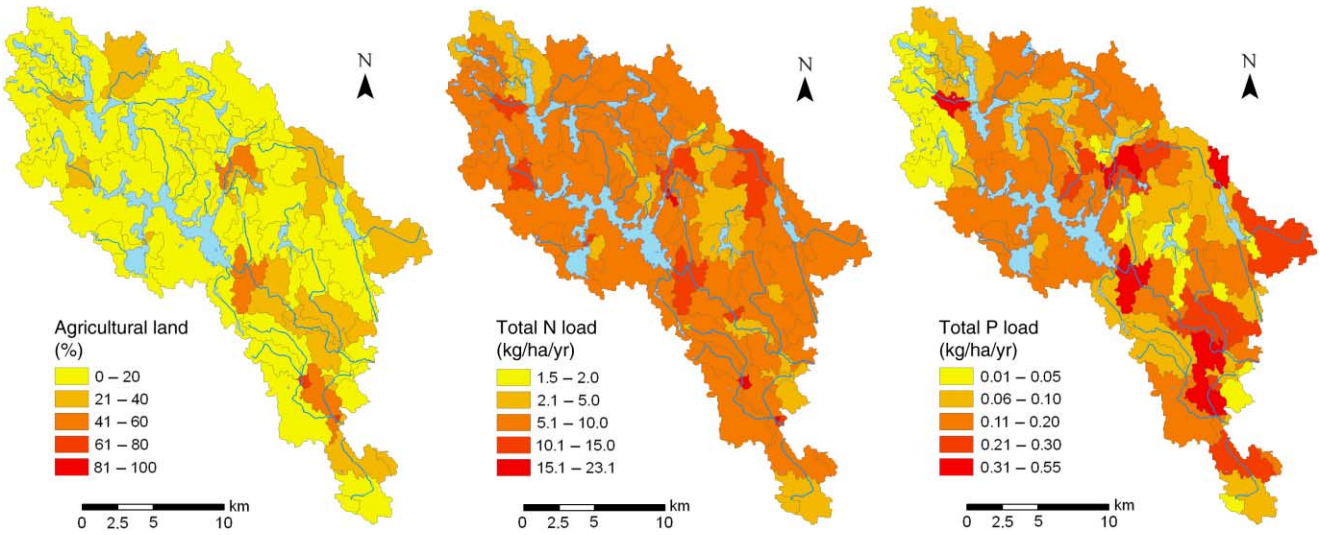


**Figure 9** | Left: percentage agricultural land; centre: average simulated loads in the local runoff from land classes of total nitrogen; and right: total phosphorus.

model fulfilled the requests (Table 2) of a fully integrated seamless model. The models in Table 2 are the most commonly used water quality models in Europe on a catchment scale. For the sake of comparison, the HBV-NP model was also included in the table.

The SWAT model (Arnold & Fohrer 2005), for instance, uses the curve number technique and the model does not have a specific lake routine. These are disadvantages for applications in Sweden, where curve numbers have not been established and there are about 100,000 lakes. The INCA model family (e.g. Wade *et al.* 2002*b*) has been developed to simulate many substances in different parts of Europe, such as N, P, C and sediments. However, the hydrological part is not complete; there is a need for a time series on effective precipitation, which is why it often uses input data from another hydrological model. INCA focuses on the riverine part of the water system and is less detailed regarding the soil turnover processes. MIKE Basin is a commercial product from DHI, based on the NAM model (Nielsen & Hansen 1973). It has an advanced user interface and is frequently used by practitioners, but the description of nutrient transformation is rather simple. MONERIS is a static source apportionment model describing flow paths (Behrendt *et al.* 2002). It is mainly based on regression analysis without detailed process descriptions. There is no water balance and observed discharge is used as an input to the model.

The HYPE model will be used for predictions in un-gauged basins for scenario modelling and climate change impact assessment. It includes relevant process descriptions and a complete hydrological model, capable of describing major hydrological features in Sweden, integrated with nutrient turnover.

**Table 2** | Characteristics of the HYPE model versus other commonly used water quality models in Europe

| Model | Full water balance | All water compartments | Full soil nutrient balance | Dynamic |
|---|---|---|---|---|
| HYPE | Yes | Yes | Yes | Yes |
| HBV-NP | Yes | Yes | No | Yes |
| INCA | No | No | No | Yes |
| MIKE BASIN | Yes | Yes | No | Yes |
| MONERIS | No | Yes | Yes | No |
| SWAT (SWIM) | Yes | No | Yes | Yes |

## Experiences from the working process

Beginning the model development with large-scale processes in low spatial resolution and then gradually increasing the detail in both space and processes was found to be a fruitful approach. The division between the modelling system and the model made it easy to formulate and test different models. Campaign measurements provide a means of evaluation, calibration and increased confidence in the

model. Although the intention was to keep the model as simple as possible, it became quite detailed due to the large number of processes needed.

### Future development

We are continuing to develop a high-resolution HYPE application for all of Sweden, according to the application of the EU Water Framework Directive. The set-up comprises more than 17,000 sub-basins corresponding to a spatial resolution of about 25 $km^2$, although it is anticipated that the spatial resolution will gradually be refined over time. The HYPE model is being integrated into the HOME Vatten system at the SMHI, where it is linked to a coastal model for user interactive simulation of eutrophication scenarios around the Swedish coast. HYPE will also become a part of the SMHI automatic production system, and simulations will therefore be available for forecast purposes.

The future applications and evaluations of the model will guide us in determining which parts of the model need refinement. All models are simplifications, but some simplifications will be more serious than others in relation to the objectives of the model applications. Some particular routines of the model that are likely to need further development are e.g. the surface runoff, processes in the riparian zone and processes during flooding of agricultural land. Furthermore, it is important to evaluate the ability of the model to successfully simulate conditions outside the range of calibration. The evaluation of independent gauging stations, as in the parameter transferability tests in this paper, is a first step but is not sufficient in this respect. Our intention is that the HYPE model will be a plausible candidate for scenario analysis, but an ensemble of models (e.g. Huisman *et al.* 2009) should preferably be used if scenario simulations are to be employed as the basis for important decisions.

## CONCLUSIONS

A first HYPE model has been developed for Swedish conditions, containing descriptions of both water flow and coupled nutrient flow and transformation. We have provided examples illustrating that the HYPE model can be calibrated to:

- provide good simulations of internal hydrological variables such as snowpack, lake water levels, soil frost depth, ground water levels and evapotranspiration;
- provide good simulations of discharge, nitrogen and phosphorus concentrations and $^{18}O$ content at catchment outlets; and
- describe much of the spatial variability in nutrient concentrations within a catchment and along a river reach.

Satisfactory simulation results were obtained when these calibrated parameter values were thereafter transferred to independent basins and lakes (at least within southern Sweden). This is by no means a complete validation of the model, but a promising first step. We intend to identify the need for further model improvements through on-going applications and evaluations of the model.

## ACKNOWLEDGEMENTS

The development of the HYPE model was mainly financed by the Swedish Meteorological and Hydrological Institute (SMHI). The project also benefited from cooperation with projects financed by the Geological Survey of Sweden (SGU) and the Swedish Research Council Formas.

## REFERENCES

Andersson, L. & Lepistö, A. 1998 Links between runoff generation, climate and nitrate-N leaching from forested catchments. *Water Air Soil Pollut.* **105**, 227–237.

Andersson, L., Rosberg, J., Pers, B. C., Olsson, J. & Arheimer, B. 2005 Estimating catchment nutrient flow with the HBV-NP model: sensitivity to input data. *Ambio* **34**, 521–532.

Andersson, L., Alkan Olsson, J., Arheimer, B. & Jonsson, A. 2008 Use of participatory scenario modelling as a platform in stakeholder dialogues. *Water SA* **34**(3), 439–447.

Arheimer, B. & Brandt, M. 1998 Modelling nitrogen transport and retention in the catchments of southern Sweden. *Ambio* **27**, 471–480.

Arheimer, B., Löwgren, M., Pers, B. C. & Rosberg, J. 2005 Integrated catchment modeling for nutrient reduction: scenarios showing impacts, potential and cost of measures. *Ambio* **34**, 513–520.

Arnold, J. G. & Fohrer, N. 2005 SWAT2000: current capabilities and research opportunities in applied watershed modelling. *Hydrol. Process.* **19**, 563–572.

Behrendt, H., Kornmilch, M., Opitz, D., Schmoll, O. & Scholz, G. 2002 Estimation of the nutrient inputs into river systems-experience from German rivers. *Reg. Environ. Changes* **3**, 107–117.

Bergström, S. 1976 Development and application of a conceptual runoff model for Scandinavian catchments. SMHI Reports RHO, No. 7, Norrköping.

Bergström, S. 1991 Principles and confidence in hydrological modelling. *Nordic Hydrol.* **22**, 123–136.

Beven, K. 2001 *Rainfall-Runoff Modelling: The Primer*. Wiley, Chichester, UK.

Bouraoui, F., Grizzetti, B., Adelskjöld, G., Behrendt, H., de Miguel, I., Silgram, M., Gómez, S., Granlund, K., Hoffmann, L., Kronvang, B., Kvaerno, S., Lázár, A., Mimikou, M., Passarella, G., Panagos, P., Reisser, H., Schwarzl, B., Siderius, C., Sileika, A. S., Smit, A. A. M. F. R., Sugrue, R., VanLiedekerke, M. & Zaloudik, J. 2009 Basin characteristics and nutrient losses: the EUROHARP catchment network perspective. *J. Environ. Monit.* **11**, 515–525.

Brandt, M. & Ejhed, H. 2002 TRK Transport–Retention–Källfördelning. Belastning på havet. (TRK Transport–Retention–Source Apportionment. Load on the sea, in Swedish). Naturvårdsverket Rapport 5247.

Brandt, M., Ejhed, H. & Rapp, L. 2008 *Näringsbelastningen på Östersjön och Västerhavet 2006. Sveriges underlag till HELCOMs femte Pollution Load Compilation* (Nutrient load on the Baltic and Western Sea. Swedish contribution to the HELCOM fifth Pollution Load Compilation, in Swedish). Swedish Environmental Protection Agency, Report 5815. p. 95.

Dean, S., Freer, J., Beven, K., Wade, A. J. & Butterfield, D. 2009 Uncertainty assessment of a process-based integrated catchment model of phosphorus. *Stochast. Environ. Res. Risk Assess.* **23**(7), 991–1010.

Eriksson, J., Andersson, A. & Andersson, R. 1997 *Tillståndet i svensk åkermark*. (The state of Swedish agricultural soils, in Swedish). Naturvårdsverket Rapport 4778.

Flügel, W. 1995 Delineating hydrological response units by geographical information-system analyses for regional hydrological modeling using PRMS/MMS in the drainage-basin of the River Brol, Germany. *Hydrol. Process.* **9**, 423–436.

Grelle, A. 2008 Achim Grelle, Department of Ecology, Swedish Agricultural University, Uppsala, Sweden (Personal Communication).

Groenendijk, P. & Kroes, J. G. 1999 *Modelling the nitrogen and phosphorus leaching to groundwater and surface water with ANIMO 3.5.* Winand Staring Centre. Wageningen (The Netherlands), Report 144.

Huisman, J. A., Breuer, L., Bormann, H., Bronstert, A., Croke, B. F. W., Frede, H.-G., Gräff, T., Hubrechts, L., Jakeman, A. J., Kite, G., Lanini, J., Leavesley, G., Lettenmaier, D. P., Lindström, G., Seibert, J., Sivapalan, M., Viney, N. R. & Willems, P. 2009 Assessing the impact of land use change on hydrology by ensemble modeling (LUCHEM) III: scenario analysis. *Adv. Water Resour.* **32**, 159–170.

Johansson, B. 2002 Estimation of areal precipitation for hydrological modelling in Sweden. Earth Sciences Centre, Department of Physical Geography, Göteborg University. Doctoral Thesis A76.

Johnsson, H., Bergström, L., Jansson, P.-E. & Paustian, K. 1987 Simulated nitrogen dynamics and losses in a layered agricultural soil. *Agric. Ecosyst. Environ.* **18**, 333–356.

Kronvang, B., Behrendt, H., Andersen, H. E., Arheimer, B., Barr, A., Borgvang, S. A., Bouraoui, F., Granlund, K., Grizzetti, B., Groenendijk, P., Schwaiger, E., Hejzlar, J., Hoffman, L., Johnsson, H., Panagopoulos, Y., Lo Porto, A, Reisser, H., Schoumans, O., Anthony, S., Silgram, M., Venohr, M. & Larsen, S. E. 2009 Ensemble modelling of nutrient loads and nutrient load partitioning in 17 European catchments. *J. Environ. Monit.* **11**, 572–583.

Krysanova, V., Hatterman, F. & Wechsung, F. 2005 Development of the ecohydrological model SWIM for regional impact studies and vulnerability assessment. *Hydrol. Process.* **19**, 763–783.

Kyllmar, K. 2004 Nitrogen leaching in small agricultural catchments. Modelling and monitoring for assessing state, trends and effects of counter-measures. Swedish University of Agricultural Sciences Agraria 485.

Lidén, R. 1999 A new approach for estimating suspended sediment yield. *Hydrol. Earth Syst. Sci.* **3**, 285–294.

Lindström, G., Johansson, B., Persson, M., Gardelin, M. & Bergström, S. 1997 Development and test of the distributed HBV-96 model. *J. Hydrol.* **201**, 272–288.

Lindström, G., Bishop, K. & Ottosson-Löfvenius, M. 2002 Soil frost and runoff at Svartberget, northern Sweden-measurements and model analysis. *Hydrol. Process.* **16**, 3379–3392.

Lindström, G., Rosberg, J. & Arheimer, B. 2005 Parameter precision in the HBV-NP model and impacts on nitrogen scenario simulations in the Rönneå River, Southern Sweden. *Ambio* **34**, 533–537.

Morgan, R. P. C. 2001 A simple approach to soil loss prediction: a revised Morgan–Morgan–Finney model. *Catena* **44**, 305–322.

Nielsen, S. A. & Hansen, E. 1973 Numerical simulation of the rainfall-runoff process on a daily basis. *Nordic Hydrol.* **4**, 171–190.

Pers, C., Lindström, G. Rosberg, J., Arheimer, B. & Andersson, L. 2006 Development of a new distributed hydrological model for large-scale and small-scale applications, In: Refsgaard, J. C. & Höjberg, A. L. (eds) *Proceedings of the XXIV Nordic Hydrological Conference*. NHP Report No. 49, pp. 307–314.

Schoumans, O., Silgram, M., Groenendijk, P., Bouraoui, F., Andersen, H. E., Kronvang, B., Behrendt, H., Arheimer, B., Johnsson, H., Panagopoulos, Y., Mimikou, M., Lo Porto, A., Reisser, H., Le Gall, G., Barr, A. & Anthony, S. G. 2009 Description of nine nutrient loss models: capabilities and suitability based on their characteristics. *J. Environ. Monit.* **11**, 506–514.

Seibert, J. & McDonell, J. J. 2002 On the dialog between experimentalist and modeler in catchment hydrology: use of soft data for multicriteria model calibration. *Water Resour. Res.* **38**(11), 1241.

Silgram, M., Schoumans, O. F., Walvoort, D. J. J., Anthony, S. G., Groenendijk, P., Strömqvist, J., Bouraoui, F., Arheimer, B., Kapetanaki, M., Lo Porto, A. & Mårtensson, K. 2009 Subannual models for catchment management: evaluating model performance on three European catchments. *J. Environ. Monit.* **11**, 526–539.

Singh, V. (ed.) 1995 *Computer Models of Watershed Hydrology*. Water Resources Publications, Littleton, Colorado.

Tattari, S., Bärlund, I., Rekolainen, S., Posch, M., Siimes, K., Thukanen, H.-R. & Yli-Halla, M. 2001 Modeling sediment yield and phosphorus transport in Finnish clayey soils. *Trans. ASAE* **44**, 297–307.

Wade, A. J., Whitehead, P. G. & O'Shea, L. C. M. 2002*a* The prediction and management of aquatic nitrogen pollution across Europe: an introduction to the Integrated Nitrogen in European Catchments project (INCA). *Hydrol. Earth Syst. Sci.* **6**, 299–313.

Wade, A. J., Durand, P., Beaujouan, V., Wessel, W. W., Raat, K. J., Whitehead, P. G., Butterfield, D., Rankinen, K. & Lepisto, A. 2002*b* A nitrogen model for European catchments: INCA, new model structure and equations. *Hydrol. Earth Syst. Sci.* **6**, 559–582.

First received 7 January 2009; accepted in revised form 21 August 2009. Available online April 2010

## APPENDIX 1: HYPE MODEL EQUATIONS

### Equations

(1) Snow accumulation

$$q_{\mathrm{SNOW}} = P \cdot \alpha_{\mathrm{SNOW}}$$

$$\alpha_{\mathrm{SNOW}} = 1 - \frac{T_{\mathrm{CLASS}} - (p_{\mathrm{TTMP}} - p_{\mathrm{TINT}})}{2 \cdot p_{\mathrm{TINT}}} \quad \text{if} \quad p_{\mathrm{TTMP}} - p_{\mathrm{TINT}} < T_{\mathrm{CLASS}} < p_{\mathrm{TTMP}} + p_{\mathrm{TINT}}$$

$$\alpha_{\mathrm{SNOW}} = 1 \quad \text{if} \quad T_{\mathrm{CLASS}} < p_{\mathrm{TTMP}} - p_{\mathrm{TINT}}$$

$$\alpha_{\mathrm{SNOW}} = 0 \quad \text{if} \quad T_{\mathrm{CLASS}} > p_{\mathrm{TTMP}} + p_{\mathrm{TINT}}$$

$$T_{\mathrm{CLASS}} = T_{\mathrm{AIR}} - p_{\mathrm{TCALT}} \cdot c_{\Delta \mathrm{H}}$$

(2) Snowmelt

$$q_{\mathrm{MELT}} = \min(p_{\mathrm{CMLT}} \cdot (T_{\mathrm{CLASS}} - p_{\mathrm{TTMP}}), W_{\mathrm{SNOW}})$$

(3) Infiltration

$$q_{\mathrm{INF}} = (P \cdot (1 - \alpha_{\mathrm{SNOW}}) + q_{\mathrm{MELT}}) - q_{\mathrm{SR}} - q_{\mathrm{MPOR}}$$

(4) Surface runoff

$$q_{\mathrm{SR}} = p_{\mathrm{RCSR}} \cdot (P \cdot (1 - \alpha_{\mathrm{SNOW}}) + q_{\mathrm{MELT}} - p_{\mathrm{THRQ}}) \quad \text{if} \quad P \cdot (1 - \alpha_{\mathrm{SNOW}}) + q_{\mathrm{MELT}} > p_{\mathrm{THRQ}}, \quad W_{\mathrm{SOIL}}(u) > p_{\mathrm{THR}\Theta}$$

(5) Macropore flow

$$q_{\mathrm{MPOR}} = p_{\mathrm{RCMP}} \cdot (P \cdot (1 - \alpha_{\mathrm{SNOW}}) + q_{\mathrm{MELT}} - p_{\mathrm{THRQ}}) \quad \text{if} \quad P \cdot (1 - \alpha_{\mathrm{SNOW}}) + q_{\mathrm{MELT}} > p_{\mathrm{THRQ}}, \quad W_{\mathrm{SOIL}}(u) > p_{\mathrm{THR}\Theta}$$

(6) Saturated overland flow

$$q_{\mathrm{SOFL}} = \max(p_{\mathrm{RCSOF}} \cdot (W_{\mathrm{SOIL}}(u) - \alpha_{\mathrm{WC}}(u)), 0)$$

(7) Percolation

$$q_{\mathrm{PERC}} = \min(\max(W_{\mathrm{SOIL}}(i) - \alpha_{\mathrm{FC}}(i), 0), \alpha_{\mathrm{WC}}(j) - W_{\mathrm{SOIL}}(j), p_{\mathrm{MPERC}}), \quad i = u, m \quad \text{and} \quad j = m, l$$

(8) Evapotranspiration

$$q_{\mathrm{E}}(i) = 0 \quad \text{if} \quad W_{\mathrm{SOIL}}(i) - \alpha_1 < 0, \quad i = u, m$$

$$q_{\mathrm{E}}(i) = \min(\alpha_{\mathrm{EVAP}}(i) \cdot E_{\mathrm{POT}}, W_{\mathrm{SOIL}}(i) - \alpha_1) \quad \text{if} \quad W_{\mathrm{SOIL}}(i) - \alpha_1 > p_{\mathrm{LP}} \cdot p_{\Theta 2} \cdot c_{\mathrm{SLAY}} \cdot 10^3, \quad i = u, m$$

$$q_{\mathrm{E}}(i) = \min\left(\alpha_{\mathrm{EVAP}}(i) \cdot E_{\mathrm{POT}} \cdot \frac{W_{\mathrm{SOIL}}(i) - \alpha_1}{p_{\mathrm{LP}} \cdot p_{\Theta 2} \cdot c_{\mathrm{SLAY}} \cdot 10^3}, W_{\mathrm{SOIL}}(i) - \alpha_1\right) \quad \text{if} \quad 0 < W_{\mathrm{SOIL}}(i) - \alpha_1 < p_{\mathrm{LP}} \cdot p_{\Theta 2} \cdot c_{\mathrm{SLAY}} \cdot 10^3, \quad i = u, m$$

$$E_{\mathrm{POT}} = p_{\mathrm{CEVP}} \cdot (T_{\mathrm{CLASS}} - p_{\mathrm{TTMP}}) \cdot \left(1 + p_{\mathrm{CEAM}} \cdot \sin\left(2 \cdot \pi \cdot \frac{t_{\mathrm{DNO}} - p_{\mathrm{CEPH}}}{365}\right)\right) \quad \text{if} \quad T_{\mathrm{CLASS}} > p_{\mathrm{TTMP}}$$

$$\alpha_{\mathrm{EVAP}}(u) = \frac{c_{\mathrm{SLAY}}(u) \cdot e^{(-p_{\mathrm{CED}} \cdot c_{\mathrm{SLAY}}(u)/2)}}{c_{\mathrm{SLAY}}(u) \cdot e^{(-p_{\mathrm{CED}} \cdot c_{\mathrm{SLAY}}(u)/2)} + c_{\mathrm{SLAY}}(m) \cdot e^{(-p_{\mathrm{CED}} \cdot (c_{\mathrm{SLAY}}(u) + c_{\mathrm{SLAY}}(m)/2))}}; \quad \alpha_{\mathrm{EVAP}}(m) = 1 - \alpha_{\mathrm{EVAP}}(u)$$

(9) Soil runoff

$$q_{\mathrm{RUNF}} = \alpha_{\mathrm{RC}} \cdot (W_{\mathrm{SOIL}} - \alpha_{\mathrm{FC}}) \quad \text{if} \quad W_{\mathrm{SOIL}} - \alpha_{\mathrm{FC}} > 0 \quad \text{(for all soil layers above soil layer with stream)}$$

$$q_{\mathrm{RUNF}} = \alpha_{\mathrm{RC}} \cdot \left((W_{\mathrm{SOIL}} - \alpha_{\mathrm{FC}}) - p_{\Theta 3} \cdot c_{\mathrm{SLAY}} \cdot 10^3 \cdot (1 - c_{\mathrm{STRD}}/c_{\mathrm{SLAY}})\right) \quad \text{if}$$
$$\left((W_{\mathrm{SOIL}} - \alpha_{\mathrm{FC}}) - p_{\Theta 3} \cdot c_{\mathrm{SLAY}} \cdot 10^3 \cdot (1 - c_{\mathrm{STRD}}/c_{\mathrm{SLAY}})\right) > 0 \quad \text{(for soil layer with stream)}$$

$$\alpha_{\mathrm{RC}}(u) = p_{\mathrm{RCU}} + p_{\mathrm{RCSL}} \cdot c_{\mathrm{SLOPE}}$$

$$\alpha_{\mathrm{RC}}(m) = \alpha_{\mathrm{RC}}(u) \cdot e^{(-\alpha_{\mathrm{ERC}} \cdot (c_{\mathrm{SLAY}}(u) + c_{\mathrm{SLAY}}(m))/2)}$$

$$\alpha_{\mathrm{RC}}(l) = p_{\mathrm{RCL}}$$

$$\alpha_{\mathrm{ERC}} = \frac{\ln(\alpha_{\mathrm{RC}}(u)/p_{\mathrm{RCL}})}{c_{\mathrm{SLAY}}(u)/2 + c_{\mathrm{SLAY}}(m) + c_{\mathrm{SLAY}}(l)/2}$$

(10) Tile drainage

$$q_{\mathrm{TILE}} = \max\left(\min\left(p_{\mathrm{RCT}} \cdot \frac{d_{\mathrm{TILE}}}{c_{\mathrm{SLAY}}} \cdot \alpha_3, W_{\mathrm{SOIL}} - \alpha_{\mathrm{FC}}\right), 0\right) \quad \text{(for soil layer with tile)}$$

(11) Regional groundwater flow

$$q_{\mathrm{GRW}} = p_{\mathrm{RCG}} \cdot (W_{\mathrm{SOIL}}(l) - \alpha_{\mathrm{FC}})$$

$$Q_{\mathrm{GRW}} = \sum_{\forall \text{ land class}} q_{\mathrm{GRW}} \cdot c_{\mathrm{AREA}}$$

(12) River delay and damping

$$Q_{\mathrm{DELAY}} = (1 - t_{\mathrm{TRPART}}) \cdot Q_{\mathrm{INFL}}(t_{\mathrm{TRDAY}}) + t_{\mathrm{TRPART}} \cdot Q_{\mathrm{INFL}}(t_{\mathrm{TRDAY}} + 1)$$

$$t_{\mathrm{TR}} = t_{\mathrm{TRDAY}} + t_{\mathrm{TRPART}} = (1 - p_{\mathrm{DAMP}}) \cdot t_{\mathrm{DELAY}}; \quad t_{\mathrm{DELAY}} = \frac{l_{\mathrm{RIV}}}{p_{\mathrm{RIVVEL}} \cdot 86,400}; \quad l_{\mathrm{RIV}} = \sqrt{\sum_{\forall \text{ land class}} c_{\mathrm{AREA}}}$$

$$Q_{\mathrm{RIV}} = \frac{\alpha_{\mathrm{DAMP}} \cdot V_{\mathrm{RIV}}}{86,400}$$

$$\alpha_{\mathrm{DAMP}} = 1 - t_{\mathrm{DAMP}} + t_{\mathrm{DAMP}} \cdot \exp\left(-\frac{1}{t_{\mathrm{DAMP}}}\right); \quad t_{\mathrm{DAMP}} = p_{\mathrm{DAMP}} \cdot t_{\mathrm{DELAY}}$$

(13) Lake outflow

$$Q_{\mathrm{LAKE}} = p_{\mathrm{K}} \cdot (W_{\mathrm{LAKE}} - c_{\mathrm{LAKED}})^{p_{\mathrm{E}}} \quad \text{if} \quad W_{\mathrm{LAKE}} > c_{\mathrm{LAKED}}, c_{\mathrm{K}} = 0$$

$$Q_{\mathrm{LAKE}} = c_{\mathrm{K}} \cdot (W_{\mathrm{LAKE}} - c_{\mathrm{W0}})^{c_{\mathrm{E}}} \quad \text{if} \quad W_{\mathrm{LAKE}} > c_{\mathrm{WHIGH}}, c_{\mathrm{K}} > 0$$

$$Q_{\mathrm{LAKE}} = c_{\mathrm{QAVG}} \cdot \left(1 + c_{\mathrm{LAMP}} \cdot \sin\left(2 \cdot \pi \cdot \frac{t_{\mathrm{DNO}} - 102}{365}\right)\right) \quad \text{if} \quad c_{\mathrm{LAKED}} < W_{\mathrm{LAKE}} < c_{\mathrm{WHIGH}}, c_{\mathrm{K}} > 0$$

$$c_{\mathrm{W0}} = c_{\mathrm{WHIGH}} - \left(\frac{c_{\mathrm{QHIGH}}}{c_{\mathrm{K}}}\right)^{1/c_{\mathrm{E}}}$$

(14) Soil pool transformation processes

$$F_{\mathrm{DEGN}} = p_{\mathrm{DEGN}} \cdot X_{\mathrm{SLOWN}} \cdot f(T_{\mathrm{SOIL}}) \cdot f(\Theta)$$

$$F_{\mathrm{MINN}} = p_{\mathrm{MINN}} \cdot X_{\mathrm{FASTN}} \cdot f(T_{\mathrm{SOIL}}) \cdot f(\Theta)$$

$$F_{\mathrm{DEGP}} = p_{\mathrm{DEGP}} \cdot X_{\mathrm{SLOWP}} \cdot f(T_{\mathrm{SOIL}}) \cdot f(\Theta)$$

$$F_{\mathrm{SOLP}} = p_{\mathrm{SOLP}} \cdot X_{\mathrm{FASTP}} \cdot f(T_{\mathrm{SOIL}}) \cdot f(\Theta)$$

$$F_{\mathrm{DENIT}} = p_{\mathrm{DENIT}} \cdot X_{\mathrm{IN}} \cdot f(T_{\mathrm{SOIL}}) \cdot f_2(\Theta) \cdot f(C_{\mathrm{IN}})$$

$$f(T_{\mathrm{SOIL}}) = \begin{cases} 2^{(T_{\mathrm{SOIL}}-20)/10} & T_{\mathrm{SOIL}} > 5^{\circ} \\ \frac{2^{(T_{\mathrm{SOIL}}-20)/10}}{5} & 0^{\circ} < T_{\mathrm{SOIL}} \leq 5^{\circ} \\ 0 & T_{\mathrm{SOIL}} \leq 0^{\circ} \end{cases}$$

$$T_{\mathrm{SOIL}}(t) = T_{\mathrm{SOIL}}(t-1) \cdot \left(1 - \frac{1}{c_{\mathrm{SOILMEM}} + c_{\mathrm{SPFROST}} \cdot d_{\mathrm{SNOW}}} - c_{\mathrm{WDEEP}}\right) + T_{\mathrm{AIR}} \cdot \frac{1}{c_{\mathrm{SOILMEM}} + c_{\mathrm{SPFROST}} \cdot d_{\mathrm{SNOW}}} + c_{\mathrm{TDEEP}} \cdot c_{\mathrm{WDEEP}}$$

$$d_{\mathrm{SNOW}} = \frac{0.1 \cdot W_{\mathrm{SNOW}}}{p_{\mathrm{DENS0}} + p_{\mathrm{DENSDT}} \cdot a_{\mathrm{SNOW}}}; \quad a_{\mathrm{SNOW}}(t) = \frac{W_{\mathrm{SNOW}}(t-1) \cdot (a_{\mathrm{SNOW}}(t-1) + 1) + q_{\mathrm{SNOW}} \cdot 0}{W_{\mathrm{SNOW}}(t)}$$

$$f(\Theta) = \begin{cases} p_{\mathrm{SATACT}} & \Theta = \Theta_{\mathrm{SAT}} \\ \min\left(\left(\frac{\Theta_{\mathrm{SAT}} - \Theta}{p_{\mathrm{RUPP}}}\right)^{p_{\mathrm{SMEX}}} \cdot (1 - p_{\mathrm{SATACT}}) + p_{\mathrm{SATACT}}, \left(\frac{\Theta - p_{\Theta 1}}{p_{\mathrm{RLOW}}}\right)^{p_{\mathrm{SMEX}}}\right) & p_{\Theta 1} \leq \Theta < \Theta_{\mathrm{SAT}} \\ 0 & \Theta < p_{\Theta 1} \end{cases}$$

$$f_2(\Theta) = \begin{cases} ((\Theta/\Theta_{\mathrm{SAT}}) - p_{\mathrm{SMDEN}})/(1 - p_{\mathrm{SMDEN}}))^{p_{\mathrm{DENEX}}} & \Theta \geq p_{\mathrm{SMDEN}} \\ 0 & \Theta < p_{\mathrm{SMDEN}} \end{cases}$$

$$\Theta_{\mathrm{SAT}} = p_{\Theta 1} + p_{\Theta 2} + p_{\Theta 3}$$

$$f(C_{\mathrm{IN}}) = \frac{C_{\mathrm{IN}}}{C_{\mathrm{IN}} + p_{\mathrm{HSATIN}}}$$

(15) Dissolved organic nitrogen in soil solution

$$F_{\mathrm{ONDI}} = p_{\mathrm{ONDI}} \cdot (p_{\mathrm{ONCO}} \cdot C_{\mathrm{ONEQ}} \cdot c_{\mathrm{SLAY}} - X_{\mathrm{FASTN}})$$

(16) Phosphorus adsorption/desorption in soil

$$F_{\mathrm{PADS}} = p_{\mathrm{PADS}} \cdot (p_{\mathrm{FRCO}} \cdot (C_{\mathrm{SPEQ}})^{p_{\mathrm{FREX}}} \cdot c_{\mathrm{SLAY}} \cdot c_{\mathrm{BULKD}} - X_{\mathrm{PARTP}})$$

(17) Plant uptake

$$F_{\mathrm{PUTN}} = \min(\alpha_{\mathrm{PUT}}, 0.8 \cdot X_{\mathrm{IN}})$$

$$F_{\mathrm{PUTP}} = \min(p_{\mathrm{PNRAT}} \cdot \alpha_{\mathrm{PUT}}, 0.8 \cdot X_{\mathrm{SP}})$$

$$\alpha_{\mathrm{PUT}} = \frac{p_{\mathrm{PUT1}} \cdot p_{\mathrm{PUT3}} \cdot \left(\frac{p_{\mathrm{PUT1}} - p_{\mathrm{PUT2}}}{p_{\mathrm{PUT2}}}\right) \cdot e^{-p_{\mathrm{PUT3}} \cdot (t_{\mathrm{DNO}} - c_{\mathrm{BD2}})}}{\left(1 + \left(\frac{p_{\mathrm{PUT1}} - p_{\mathrm{PUT2}}}{p_{\mathrm{PUT2}}}\right) \cdot e^{-p_{\mathrm{PUT3}} \cdot (t_{\mathrm{DNO}} - c_{\mathrm{BD2}})}\right)^2}$$

$$\alpha_{\mathrm{PUT}} = \alpha_{\mathrm{PUTAUT}} \text{ if } t_{\mathrm{DNO}} > c_{\mathrm{BD5}}$$

$$\alpha_{\mathrm{PUTAUT}} = \frac{p_{\mathrm{PUT1}} \cdot p_{\mathrm{PUT3}} \cdot \left(\frac{p_{\mathrm{PUT1}} - p_{\mathrm{PUT2}}}{p_{\mathrm{PUT2}}}\right) \cdot e^{-p_{\mathrm{PUT3}} \cdot (t_{\mathrm{DNO}} - c_{\mathrm{BD5}} - 25)}}{\left(1 + \left(\frac{p_{\mathrm{PUT1}} - p_{\mathrm{PUT2}}}{p_{\mathrm{PUT2}}}\right) \cdot e^{-p_{\mathrm{PUT3}} \cdot (t_{\mathrm{DNO}} - c_{\mathrm{BD5}} - 25)}\right)^2} \cdot f(T_{\mathrm{AIR}})$$

$$f(T_{\mathrm{AIR}}) = \begin{cases} 0 & T_{\mathrm{AIR}} < p_{\mathrm{TTHR}} \\ \min\left(1, \left(\frac{1}{p_{\mathrm{TMAX}} - p_{\mathrm{TTHR}}}\right) \cdot T_{\mathrm{AIR}} - \frac{p_{\mathrm{TTHR}}}{p_{\mathrm{TMAX}} - p_{\mathrm{TTHR}}}\right) & T_{\mathrm{AIR}} \geq p_{\mathrm{TTHR}} \end{cases}$$

(18) Soil erosion of phosphorous and transport to river

$$F_{\mathrm{PPRIV}} = X_{\mathrm{PPINT}} \cdot \max(1, (q_{\mathrm{RUNF}} / p_{\mathrm{TPP1}})^{p_{\mathrm{TPP2}}})$$

$$F_{\mathrm{PPTR}} = 10^{-3} \cdot \alpha_{\mathrm{ENRICH}} \cdot (F_{\mathrm{DETRF}} + F_{\mathrm{DETOF}}) \cdot \frac{(X_{\mathrm{SLOWP}} + X_{\mathrm{PARTP}})}{(c_{\mathrm{SLAY}} \cdot c_{\mathrm{BULKD}})} \cdot \max(1, ((q_{\mathrm{SR}} + q_{\mathrm{SOFL}} + q_{\mathrm{MPOR}}) / p_{\mathrm{TR1}})^{p_{\mathrm{TR2}}})$$

$$\alpha_{\mathrm{ENRICH}} = \begin{cases} p_{\mathrm{STAB}} & q_{\mathrm{SR}} + q_{\mathrm{SOFL}} + q_{\mathrm{MPOR}} > p_{\mathrm{QSTAB}} \\ \frac{p_{\mathrm{MAXQ}} - (p_{\mathrm{MAXQ}} - p_{\mathrm{STAB}}) \cdot (q_{\mathrm{SR}} + q_{\mathrm{SOFL}} + q_{\mathrm{MPOR}})}{p_{\mathrm{QSTAB}}} & q_{\mathrm{SR}} + q_{\mathrm{SOFL}} + q_{\mathrm{MPOR}} \leq p_{\mathrm{QSTAB}} \\ 0 & q_{\mathrm{SR}} + q_{\mathrm{SOFL}} + q_{\mathrm{MPOR}} = 0 \end{cases}$$

$$F_{\mathrm{DETRF}} = \alpha_{\mathrm{KE}} \cdot P \cdot p_{\mathrm{EROD}} \cdot (1 - \alpha_{\mathrm{CC}})$$

$$F_{\mathrm{DETOF}} = ((q_{\mathrm{SR}} + q_{\mathrm{SOFL}}) \cdot 365)^{p_{\mathrm{OFDET}}} \cdot (1 - \alpha_{\mathrm{GC}}) \cdot \left(\frac{1}{0.5 \cdot p_{\mathrm{COH}}}\right) \cdot \sin(c_{\mathrm{SLOPE}}) / 365$$

$$\alpha_{\mathrm{KE}} = 8.95 + 8.44 \cdot \log_{10}(p_{\mathrm{INTR}})$$

(19) Sedimentation and resuspension in lakes and rivers

$$F_{\mathrm{SEDON}} = 10^{-3} \cdot p_{\mathrm{SEDON}} \cdot C_{\mathrm{ON}} \cdot c_{\mathrm{AREA}}$$

$$F_{\mathrm{SEDPPL}} = 10^{-3} \cdot p_{\mathrm{SEDPPL}} \cdot C_{\mathrm{PP}} \cdot c_{\mathrm{AREA}}$$

$$F_{\mathrm{SEDPPR}} = 10^{-3} \cdot \left( \frac{Q_{\mathrm{RIV}} - Q_{\mathrm{BANK}}}{Q_{\mathrm{BANK}}} \right)^{p_{\mathrm{SEDEX}}} \cdot C_{\mathrm{PP}} \cdot l_{\mathrm{RIV}} \cdot w_{\mathrm{RIV}} \cdot d_{\mathrm{RIV}}$$

$$F_{\mathrm{RESPPR}} = \left( \frac{Q_{\mathrm{RIV}}}{Q_{\mathrm{BANK}}} \right)^{p_{\mathrm{SEDEX}}} \cdot X_{\mathrm{SEDPP}}$$

$$w_{\mathrm{RIV}} = 10^{p_{\mathrm{RIV4}}} \cdot \left( \frac{Q_{\mathrm{RIV}}}{v_{\mathrm{RIV}}} \right)^{\left( p_{\mathrm{RIV5}} + p_{\mathrm{RIV6}} \log_{10} \left( \frac{Q_{\mathrm{RIV}}}{v_{\mathrm{RIV}}} \right) \right)}; \qquad v_{\mathrm{RIV}} = 10^{p_{\mathrm{RIV1}}} \cdot \bar{Q}^{p_{\mathrm{RIV2}}} \cdot \left( \frac{Q_{\mathrm{RIV}}}{\bar{Q}} \right)^{p_{\mathrm{RIV3}}}; \qquad d_{\mathrm{RIV}} = \left( \frac{Q_{\mathrm{RIV}}/v_{\mathrm{RIV}}}{w_{\mathrm{RIV}}} \right)$$

(20) Primary production, mineralization and denitrification in lakes and rivers

$$F_{\mathrm{PRODNW}} = p_{\mathrm{PROMIN}} \cdot f(T_{\mathrm{WATER}}) \cdot f(T_{10}, T_{20}) \cdot f(\bar{C}_{\mathrm{TP}}) \cdot V_{\mathrm{RIV/LAKE}}$$

$$F_{\mathrm{PRODPW}} = p_{\mathrm{NPRAT}} \cdot F_{\mathrm{PRODNW}}$$

$$F_{\mathrm{MINNW}} = -F_{\mathrm{PRODNW}}$$

$$F_{\mathrm{MINPW}} = -F_{\mathrm{PRODPW}}$$

$$F_{\mathrm{DENW}} = p_{\mathrm{DENW}} \cdot f(C_{\mathrm{IN}}) \cdot f(T_{\mathrm{WATER}}) \cdot c_{\mathrm{AREA}}$$

$$f(T_{\mathrm{WATER}}) = \frac{T_{\mathrm{WATER}}}{20}; \qquad T_{\mathrm{WATER}}(t) = (1 - p_{\mathrm{WAIR}}) \cdot T_{\mathrm{WATER}}(t-1) + p_{\mathrm{WAIR}} \cdot T_{\mathrm{AIR}}$$

$$f(\bar{C}_{TP}) = \frac{\bar{C}_{TP}}{\bar{C}_{TP} + p_{HSATTP}}; \qquad f(C_{\mathrm{IN}}) = \frac{C_{\mathrm{IN}}}{C_{\mathrm{IN}} + p_{\mathrm{HSATIN}}} \qquad f(T_{10}, T_{20}) = \frac{T_{10} - T_{20}}{5}$$

## APPENDIX 2: NOTATION

### State variables

| | |
|---|---|
| $C_{\mathrm{IN}}$ | concentration of inorganic nitrogen (mg/l) |
| $C_{\mathrm{ON}}$ | concentration of organic nitrogen (mg/l) |
| $C_{\mathrm{PP}}$ | concentration of particulate phosphorus (mg/l) |
| $V_{\mathrm{RIV}}$ | volume of river ($m^3$) |
| $W_{\mathrm{LAKE}}$ | water level of lake (m) |
| $W_{\mathrm{SNOW}}$ | water content of snow (mm) |
| $W_{\mathrm{SOIL}}$ | soil moisture (mm) |
| $X_{\mathrm{FASTN}}$ | fast turnover N pool (kg/$km^2$) |
| $X_{\mathrm{FASTP}}$ | fast turnover P pool (kg/$km^2$) |
| $X_{\mathrm{IN}}$ | inorganic N pool (kg/$km^2$) |
| $X_{\mathrm{PARTP}}$ | mineral P pool (kg/$km^2$) |
| $X_{\mathrm{PPINT}}$ | intermediate PP storage pool (kg/$km^2$) |
| $X_{\mathrm{SEDPP}}$ | pool of PP in river sediment (kg) |
| $X_{\mathrm{SLOWN}}$ | slow turnover N pool (kg/$km^2$) |
| $X_{\mathrm{SLOWP}}$ | slow turnover P pool (kg/$km^2$) |
| $X_{\mathrm{SP}}$ | dissolved P pool (kg/$km^2$) |

### Process variables

| | |
|---|---|
| $F_{\mathrm{DEGN}}$ | degradation of humusN (kg/$km^2$ d) |
| $F_{\mathrm{DEGP}}$ | degradation of humusP (kg/$km^2$ d) |
| $F_{\mathrm{DENIT}}$ | denitrification in soil (kg/$km^2$ d) |
| $F_{\mathrm{DENW}}$ | denitrification in lakes and rivers (kg/d) |
| $F_{\mathrm{DETOF}}$ | detachment of sediment due to overland flow (g/$m^2$ d) |
| $F_{\mathrm{DETRF}}$ | detachment of sediment due to rainfall (g/$m^2$ d) |
| $F_{\mathrm{MINN}}$ | mineralization of fastN (kg/$km^2$ d) |

$F_{MINNW}$ net mineralization of N in water (kg/d)
$F_{MINPW}$ net mineralization of P in water (kg/d)
$F_{ONDI}$ dissolution of ON nitrogen (kg/km$^2$ d)
$F_{PADS}$ adsorption/desorption of SP (kg/km$^2$ d)
$F_{PPRIV}$ transport of PP to river from intermediate pool (kg/km$^2$ d)
$F_{PPTR}$ transport of detached PP (kg/km$^2$ d)
$F_{PRODNW}$ net primary production of N in water (kg/d)
$F_{PRODPW}$ net primary production of N in water (kg/d)
$F_{PUTN}$ plant uptake of N (kg/km$^2$ d)
$F_{PUTP}$ plant uptake of P (kg/km$^2$ d)
$F_{RESPPL}$ resuspension of PP in rivers (kg/d)
$F_{SEDON}$ sedimentation of ON in lakes (kg/d)
$F_{SEDPPL}$ sedimentation of PP in lakes (kg/d)
$F_{SEDPPR}$ sedimentation of PP in rivers (kg/d)
$F_{SOLP}$ solubilization of fastP (kg/km$^2$ d)
$Q_{DELAY}$ river flow after delay (m$^3$/s)
$q_E$ evapotranspiration (mm/d)
$q_{GRW}$ regional groundwater outflow from a class (mm/d)
$Q_{GRW}$ regional groundwater outflow from a sub-basin (mm m$^2$/d)
$q_{INF}$ infiltration (mm/d)
$Q_{INFL}$ total inflow to river (m$^3$/s)
$Q_{LAKE}$ lake outflow simple lake (m$^3$/s)
$q_{MELT}$ snowmelt (mm/d)
$q_{MPOR}$ macropore flow (mm/d)
$q_{PERC}$ percolation (mm/d)
$Q_{RIV}$ river flow after damping and delay = inflow to lake (m$^3$/s)
$q_{RUNF}$ soil runoff (mm/d)
$q_{SNOW}$ snow fall (mm/d)
$q_{SOFL}$ saturated overland flow (mm/d)
$q_{SR}$ surface runoff due to excess infiltration (mm/d)
$q_{TILE}$ tile drainage runoff (mm/d)

## Other variables

$a_{SNOW}$ age of snow (d)
$C_{ONEQ}$ equilibrium concentration for ON (mg/l)
$C_{SPEQ}$ SP equilibrium concentration (mg/l)
$\bar{C}_{TP}$ mean total phosphorus concentration (mg/l)
$d_{RIV}$ river depth (m)
$d_{SNOW}$ snow depth (cm)
$d_{TILE}$ water stage above tile depth (m)
$E_{POT}$ potential evapotranspiration (mm/d)
$i$ soil layer index (u, m or l)
$j$ soil layer index (u, m or l)
$l$ lowest soil layer (–)
$l_{RIV}$ river length (m)
$m$ second soil layer (–)
$P$ precipitation (mm/d)
$\overline{Q}$ mean river flow (m$^3$/s)
$Q_{BANK}$ bank full river flow (m$^3$/s)
$t$ time step (d)
$T_{10}$ average water temperature over a 10 day period (°C)
$T_{20}$ average water temperature over a 20 day period (°C)
$T_{AIR}$ air temperature for sub-basin (°C)
$T_{CLASS}$ air temperature for class (°C)
$t_{DAMP}$ delay time in river through damping (d)
$t_{DELAY}$ total delay time in river (d)
$t_{DNO}$ day number of year (d)
$T_{SOIL}$ temperature of soil (°C)
$t_{TR}$ delay time in river through translation (d)
$t_{TRDAY}$ whole days of delay in translation (d)
$t_{TRPART}$ remaining part of delay in translation (d)
$T_{WATER}$ water temperature (°C)
$V_{LAKE}$ volume of lake (m$^3$)
$v_{RIV}$ river flow velocity (m/s)
$w_{RIV}$ river width (m)
$W_{SOIL}$ water content of soil (mm)
$u$ upper soil layer (–)
$\alpha_1$ maximum water content not available for evapotranspiration (mm)
$\alpha_3$ maximum water content available for runoff (mm)
$\alpha_{CC}$ crop cover factor (–)
$\alpha_{DAMP}$ outflow coefficient for damping (–)
$\alpha_{ENRICH}$ enrichment factor (–)
$\alpha_{ERC}$ exponential rate of runoff coefficient (1/m)
$\alpha_{EVAP}$ fraction of evapotranspiration from soil layer (–)
$\alpha_{FC}$ water content at threshold for runoff (mm)
$\alpha_{GC}$ ground cover factor (–)
$\alpha_{KE}$ kinetic energy in rainfall (J/m$^2$ mm)
$\alpha_{PUT}$ potential plant uptake (g/m$^2$ d)

$\alpha_{PUTAUT}$ potential plant uptake in autumn for autumn sown crop (g/m$^2$ d)
$\alpha_{RC}$ soil runoff coefficient (1/d)
$\alpha_{SNOW}$ snow fraction of precipitation (–)
$\alpha_{WC}$ maximum water content of soil (mm)
$\Theta$ water content of soil (–)
$\Theta_{SAT}$ water content at saturation (–)

## Model parameters

$p_{CEAM}$ amplitude of evapotranspiration seasonal correction (general) (–)
$p_{CED}$ decrease of evapotranspiration with soil depth (general) (1/m)
$p_{CEPH}$ phase of evapotranspiration seasonal correction (general) (d)
$p_{CEVP}$ rate of potential evapotranspiration (land use) (mm/d °C)
$p_{CMLT}$ snow melt coefficient (land use) (mm/d °C)
$p_{COH}$ cohesion of soil (soil type) (kPa)
$p_{DAMP}$ part of delay time in river through damping (general) (–)
$p_{DEGN}$ degradation of humus N to fast N (general) (1/d)
$p_{DEGP}$ degradation of humus P to fast P (general) (1/d)
$p_{DENEX}$ exponent in soil moisture function for denitrification (general) (–)
$p_{DENIT}$ denitrification rate in soil (general) (1/d)
$p_{DENS0}$ snow density of new snow (general) (–)
$p_{DENSDT}$ change of snow density with time (general) (1/d)
$p_{DENW}$ denitrification in water (general) (kg/m$^2$ d)
$p_{E}$ exponent of lake rating curve (general) (–)
$p_{EROD}$ erodibility of soil (soil type) (g/J)
$p_{FRCO}$ coefficient in Freundlich Equation (soil type) (1/kg)
$p_{FREX}$ exponent in Freundlich Equation (soil type) (–)
$p_{HSATIN}$ half saturation point for IN concentration (general) (mg/l)
$p_{HSATTP}$ half saturation point for TP concentration (general) (mg/l)
$p_{INTR}$ rainfall intensity (general) (mm/h)
$p_{K}$ rate of lake rating curve (general) (–)
$p_{LP}$ limit for potential evapotranspiration (general) (–)
$p_{MAXQ}$ parameter in enrichment factor calculation (general) (mm/d)
$p_{MINN}$ mineralization of fast N to IN (general) (1/d)
$p_{MPERC}$ maximum percolation (soil type) (mm/d)
$p_{NPRAT}$ NP ratio in mineralization/primary production Equation (general) (–)
$p_{OFDET}$ exponent in overland flow detachment Equation (general) (–)
$p_{ONCO}$ coefficient in linear isotherm (general) (l/m$^3$)
$p_{ONDI}$ ON dissolution rate (general) (1/d)
$p_{PADS}$ adsorption/desorption rate (soil type) (1/d)
$p_{PNRAT}$ PN ratio in plant uptake (general) (–)
$p_{PRODMIN}$ primary production mineralization parameter (general) (kg/m$^3$ d)
$p_{PUT1}$ plant uptake parameter (crop type) (g/m$^2$)
$p_{PUT2}$ plant uptake parameter (crop type) (g/m$^2$)
$p_{PUT3}$ plant uptake parameter (crop type) (1/d)
$p_{RCG}$ runoff coefficient for regional groundwater flow (general) (1/d)
$p_{RCL}$ soil runoff coefficient for lowest layer (soil type) (1/d)
$p_{RCMP}$ runoff coefficient for macropore flow (soil type) (–)
$p_{RCSL}$ runoff coefficient dependence on slope (soil type) (1/d %)
$p_{RCSOF}$ runoff coefficient for saturation overland flow (land use) (1/d)
$p_{RCSR}$ runoff coefficient for surface runoff (soil type) (–)
$p_{RCT}$ tile drainage runoff coefficient (soil type) (1/d)
$p_{RCU}$ soil runoff coefficient for top layer (soil type) (1/d)
$p_{RIV1}$, $p_{RIV2}$, $p_{RIV3}$, $p_{RIV4}$, $p_{RIV5}$, $p_{RIV6}$ empirical parameters in the river dimension Equations (lake region) (–)
$p_{QSTAB}$ flow threshold for stabilization of enrichment factor (general) (mm/d)
$p_{RIVVEL}$ river flow velocity (general) (m/s)
$p_{RLOW}$ lower range in soil moisture function (general) (–)
$p_{RUPP}$ upper range in soil moisture function (general) (–)
$p_{SATACT}$ activity at saturation (general) (–)
$p_{SEDEX}$ exponent in sedimentation/resuspension Equations (general) (–)
$p_{SEDON}$ sedimentation of ON in lakes (general) (l/km$^2$ d)
$p_{SEDPPL}$ sedimentation of PP in lakes (general) (l/km$^2$ d)
$p_{SMDEN}$ coefficient in soil moisture function for denitrification (general) (–)

$p_{SMEX}$ exponent in soil moisture function (general) (–)
$p_{SOLP}$ solubiliztion of fastP to SP (general) (1/d)
$p_{STAB}$ enrichment factor for flows above stabilization threshold (general) (–)
$p_{TCALT}$ air temperatures elevation dependence (general) (°C/m)
$p_{THRQ}$ flow threshold for surface runoff and macropore flow (soil type) (mm/d)
$p_{THR\Theta}$ soil moisture threshold for surface runoff and macropore flow (soil type) (mm)
$p_{TINT}$ half temperature interval for mixed snow and rain (general) (°C)
$p_{TMAX}$ parameter in winter crop nutrient uptake calculation (general) (°C)
$p_{TPP1}$ parameter in PP transport to rivers Equation (general) (mm/d)
$p_{TPP2}$ exponent in PP transport to rivers Equation (general) (–)
$p_{TR1}$ parameter in transport capacity Equation (general) (mm/d)
$p_{TR2}$ exponent in transport capacity Equation (general) (–)
$p_{TTMP}$ temperature threshold (land use) (°C)
$p_{TTHR}$ temperature threshold for plant nutrient uptake during late autumn (general) (°C)
$p_{WAIR}$ weight for air temperature in water temperature Equation (general) (–)
$p_{\Theta 1}$ fraction of soil layer where water is not available for evapotranspiration (soil type) (–)
$p_{\Theta 2}$ fraction of soil layer where water is available for evapotranspiration but not for runoff (soil type) (–)
$p_{\Theta 3}$ fraction of soil layer where water is available for runoff (soil type) (–)

## Constants/input data

$c_{AREA}$ class area ($m^2$)
$c_{BD2}$ day number of sowing date in spring (d)
$c_{BD5}$ day number of sowing date in autumn (d)
$c_{BULKD}$ bulk density of soil ($kg/m^3$)
$c_{E}$ exponent of regulated lake rating curve for high water levels (spilling) (–)
$c_{K}$ rate of regulated lake rating curve for high water levels (spilling) (–)
$c_{LAKED}$ depth of lake below outflow threshold (m)
$c_{LAMP}$ amplitude of seasonal variation of normal lake discharge (–)
$c_{QAVG}$ normal lake discharge ($m^3/s$)
$c_{QHIGH}$ lake discharge at high water level ($m^3/s$)
$c_{SLAY}$ soil layer thickness (m)
$c_{SLOPE}$ slope of sub-basin (%)
$c_{SOILMEM}$ soil temperature memory (30 d)
$c_{SPFROST}$ soil temperature snow dependence (10 d/cm)
$c_{STRD}$ stream depth below soil surface (m)
$c_{TDEEP}$ deep soil temperature (5°C)
$c_{TILE}$ depth of tile and drainage pipe (m)
$c_{W0}$ water level of regulated lake rating curve for high water levels (spilling) (m)
$c_{WDEEP}$ deep soil temperature weight (0.001)
$c_{WHIGH}$ high water level above which a regulated lake is spilled (m)
$c_{\Delta H}$ class' elevation deviation from sub-basin mean elevation (m)